Novel Manufacturing Method for Large Scale and Energetic Material Containing Paraffin-Based Hybrid Rocket Fuel Grains

by

Utku Can YILDIZ

A Dissertation Submitted to the

Graduate School of Sciences and Engineering

in Partial Fulfillment of the Requirements for

the Degree of

Master of Engineering

in

Mechanical Engineering

August 2023

Novel Manufacturing Method for Large Scale

and Energetic Material Containing Paraffin-Based Hybrid Rocket Fuel Grains

Koç University

Graduate School of Sciences and Engineering

This is to certify that I have examined this copy of a master's thesis by

Utku Can YILDIZ

and have found that it is complete and satisfactory in all respects,

and that any and all revisions required by the final

examining committee have been made.

Committee Members:

_____

Assoc. Prof. Mustafa Arif KARABEYOĞLU (Advisor)

_____

Prof. Dr. Onur TUNÇER

_____

Prof. Dr. Metin MURADOĞLU

Date: _____

I want to dedicate this thesis to my beloved family, my love Nur Ber EMERCE, and especially to one and only my mom, Muradiye YILDIZ. Undoubtedly, I would like to also dedicate this thesis to dear Mustafa BAYSAL, who is not only my friend but also my colleague who has profound knowledge. Finally, I want to convey my utmost respect to my thesis advisor, Assoc. Prof. Arif KARABEYOĞLU, for his support. His determination, perseverance, and vast knowledge have always been a source of inspiration for me and will continue to be.

Dear mom, it is very difficult to put into words my gratitude towards you. As I look back to my journey, you have been always my unwavering pillar of support in the time I need. Your love, encouragement, and the sacrifices you have made, have shaped me into the person I am today. As I embark on a new adventure in life, I am eternally grateful for your presence. I will always carry your love and guidance with me.

Bu tezi sevgili aileme, sevgilim Nur Ber EMERCE'ye ve özellikle birtanecik anneme, Muradiye YILDIZ'a adamak istiyorum. Şüphesiz, bu tezi sadece dostum değil, aynı zamanda engin bilgiye sahip bir meslektaşım olan sevgili Mustafa BAYSAL'a da adamak istiyorum. Son olarak, tez danışmanım Sayın Doç. Dr. Arif KARABEYOĞLU'na desteği için en derin saygılarımı sunmak istiyorum. Kendisinin kararlılığı, azmi ve engin bilgisi her zaman benim için bir ilham kaynağı olmuştur ve olmaya devam edecektir.

Sevgili anneciğim, sana olan minnettarlığımı kelimelere dökmek gerçekten zor. Geçmişime baktığımda, her ihtiyaç duyduğum anda yanımda oldun. Senin sevgin, teşvikin ve yaptığın fedakarlıklar beni bugün olduğum kişi haline getirdi. Hayatta yeni bir maceraya adım attığım şu anda, senin varlığına sonsuz minnettarım. Senin sevgini ve rehberliğini her zaman yanımda taşıyacağım.

ABSTRACT

The propulsion system designs are tailored according to the mission's requirements. Launching and sounding rockets demand high thrust, a condition feasible through the interaction of propellant and oxidizer at high flow rates. In addition to cost, safety, and operational ease considerations, high regression rate and competitive specific impulse make paraffin-based hybrid fuels a robust candidate for both launching and sounding rockets.

Centrifugal and direct casting are the standard methods to manufacture paraffin-based fuel grains. The fuel melt's composition may influence the preference for a specific production method. For instance, metallic additives in the demanded fuel formulation make the centrifugal casting method unsuitable due to phase separation between polymeric melt and metallic powder induced by density differences. It makes the direct casting method the only option. However, the direct casting method introduces deviations in the fuel grain's dimensional tolerances. It leads to a substantial reduction in both mechanical properties and density due to exposed micro defects while the melt solidifies.

This thesis aims to develop a novel fuel grain manufacturing method with distinctive advantages over classical centrifuge and direct fuel casting techniques. Additionally, it seeks to determine production parameters affecting mechanical properties, identify micro-mechanisms impacting mechanical characteristics, and elucidate specific scenarios wherein the new production method offers favorable outcomes. The fuel formulation is prepared and obtained in a liquid state in the advanced method. It is subsequently transformed into micron-sized particles by spraying into a reactor filled with inert gas through a nozzle. The resulting particles are then placed into molds designed to achieve the desired fuel grain shape and compressed using a uniaxial hydraulic system to obtain a homogeneous solid fuel grain.

Within this framework, the thesis study involved the production of over 500 kg of hybrid rocket fuel powder, evaluating more than eight distinct mold designs, and the generation of over 400 samples for the investigation of mechanical and combustion characteristics. Tensile test specimens were extracted from the produced fuel cores, and their mechanical properties and fracture surfaces were examined using an electron microscope. Finally, fuel cores prepared from different formulations tested with appropriate hybrid rocket motors. The test results demonstrate that the new fuel production method facilitates the homogeneous incorporation of metallic additives characterized by a high-density difference into the fuel melt, enabling the utilization of additives requiring processing at low temperatures as fuel. Furthermore, a new additive is proposed for paraffin-based hybrid rocket fuels. The proposed additive, blowing agent, enhance the fuel regression rate up to %178 at 60 g/cm^{2}s oxidizer flux compared to the base fuel formula’s regression rate.

ÖZETÇE

İtki sistemi tasarımları görevin isterlerine göre şekillendirilmektedir. Fırlatma roketleri ve sonda roketleri yüksek itki elde etmeyi gerektirir. Bu durum yakıt ve oksitleyicinin yüksek debilerde reaksiyona sokulması ile mümkündür. Maliyet, güvenlik, operasyon kolaylığının yanı sıra yüksek yanma hızı ve rekabetçi özgül darbe değeri, parafin bazlı hibrit yakıtları fırlatma sistemleri ve sonda roketleri için oldukça güçlü bir adaydır.

Parafin bazlı yakıt çekirdeği üretimi santrifüj yöntemi ya da direkt döküm yöntemi ile gerçekleştirilmektedir. Yakıt eriyiğinin içeriği farklı üretim yöntemi tercihine sebep olabilir. Örneğin özkütle farklılıkları sebebiyle metalik katkıya sahip bir yakıt çekirdeğinin üretimi faz ayrımı sebepli santrifüj yöntemi ile gerçekleştirilemeyeceğinden direkt döküm yöntemi ile üretilir. Ancak direkt döküm yöntemi yakıt çekirdeğinin ölçü toleranslarında sapmalara ve mekanik özelliklerin çok ciddi anlamda düşüşüne sebep olur.

Bu tezin amacı, klasik santrifüj ve direkt yakıt döküm yöntemine alternatif, kendine has avantajları olan yeni bir yakıt yöntemi geliştirmek, mekanik özellikleri etkileyen üretim parametrelerin belirlenmesi, mekanik özellikleri etkileyen mikro mekanizmaların belirlenmesi ve yeni üretim yönteminin avantaj sağlayacağı spesifik durumların ortaya konulmasıdır. Geliştirilmiş olan yöntemde yakıt formülasyonu sıvı formda hazırlanıp elde edildikten sonra bir nozül vasıtasıyla asal gaz dolu bir reaktöre püskürtülerek mikron boyutta toza dönüştürülür. Elde edilen bu toz hedeflenen yakıt çekirdeği formunda üretilmiş olan kalıba doldurularak tek eksenli bir hidrolik ile sıkıştırılır ve yekpare yakıt çekirdeği elde edilir. Bu kapsamda tez çalışması süresince 500 kg'dan fazla hibrit roket yakıt tozu üretilmiş, 8'den fazla farklı kalıp tasarımı değerlendirilmiş, mekanik ve yanma karakteristiğinin araştırılması adına 400'den fazla numune üretimi gerçekleştirilmiştir. Üretilen yakıt çekirdeklerinden çekme testi numuneleri alınmış, mekanik özellikleri ve kırılım yüzeyleri elektron mikroskobu ile incelenmiştir. Son olarak farklı formülasyonlardan hazırlanmış yakıt çekirdekleri uygun hibrit roket motorları ile test edilmiştir. Testler sonucu, yeni yakıt üretim yöntemi özellikle yakıt eriyiği ile arasında yüksek özkütle farklılığı olan metal katkıların yakıt çekirdeğine homojen bir şekilde eklenmesine imkân verdiği ve düşük sıcaklıklarda proses edilmesi gereken katkıların da bu yöntem sayesinde yakıt olarak kullanılabileceği gözlemlenmiştir. Ek olarak, yeni bir parafin-bazlı yakıt katkısı bu tezde sunulmuştur. Bahsi geçen köpürtme ajanı baz yakıt formülasyonunun yanma hızını $50 g/cm^2 s$ oksitleyici akısında %178 oranında arttırmıştır.

ACKNOWLEDGEMENTS

Throughout the study, necessary tools, financial support, required infrastructure, and test facilities are provided by DeltaV Space Technology Inc. I want to thank you to my advisor and DeltaV Space Technology President Assoc. Prof. Arif KARABEYOĞLU for giving his support in this study.

I wish to extend my special thanks to my colleagues who helped me throughout the study. Firstly, Dr. Mustafa BAYSAL has always taken his time to me for my every question with extended informative sessions. Also, my dear colleagues Nur Ber EMERCE, Uğur KOKAL, and Yiğit YILDIZ have supported me throughout working hours to take my time for the study. I also wish to thank to my dear colleague Büşra KAHRAMAN for helping me to arrange the appropriate infrastructure to conduct my propulsion tests. Finally, I thank dear Semih ÇALIŞKAN and Tuncay DUMAN for helping me to produce the required materials and conduct tests.

LIST OF TABLES

LIST OF FIGURES

ABBREVIATIONS

HRE Hybrid Rocket Engine

PW: Paraffin Wax

EVA: Ethylene Vinyl Acetate

LDPE: Low-Density Polyethylene

SEBS: Styrene-Ethylene-Butylene-Styrene

SA: Stearic Acid

PE: Polyethylene

CNTs: Carbon Nanotubes

MWCNT: Multi-Walled Carbon Nanotubes (MWCNT),

$LiAlH_4$: Lithium-Aluminum-Hydride

BH_3NH_3: Ammonia-Borane

HMOFs: Hypergolic Metal-Organic Frameworks

IPA: Isopropyl Alcohol

CC: Centrifugal Casting

S: Sintered

DC: Direct Casting

PBF: Paraffinic Base Formula

PAL40: Paraffinic Base Formula + 40% Aluminum

PBA1: Paraffinic Base Formula + 1% Blowing Agent

PBA5: Paraffinic Base Formula + 5% Blowing Agent

PBA10: Paraffinic Base Formula + 10% Blowing Agent

NOMENCLATURE

A area, m^2 *(*ft^2*)*

A_t nozzle throat area, m^2 *(*ft^2*)*

c effective velocity, m/sec (ft/sec)

$c*$ characteristic velocity, m/sec (ft/sec)

F thrust force, N (lbf)

g_0 standard sea-level acceleration of gravity,

9.80665 m/sec^2 *(*32.174 ft/sec^2*)*

I_s specific impulse, sec

It impulse or total impulse, N-sec (lbf-sec)

m mass, kg (slugs) (1 slug = mass of 32.174 lb of weight at sea level)

$\dot{m}$ mass flow rate, kg/sec (lbm/sec)

m_p propellant mass, kg (lbm or slugs)

Q_r heat of reaction per unit propellant, J/kg (Btu/lbm)

t time, sec

u vehicle velocity, m/sec (ft/sec)

w weight, N or kg-m/sec^2 (lbf)

Cd discharge coefficient %

X_c degree of crystallinity

ΔH enthalpy, J

η efficiency

η_{comb} combustion efficiency

TABLE OF CONTENTS

Chapter 1:
INTRODUCTION

Primitive versions of the rockets are observed in Chines military applications around 800 years ago; however, the first definition, like today's understanding, was done by Russian Konstantin E. Ziolkowsyk, proposing fundamental rocket flight equation to build rockets in 1903. From the 1900s to today, various rocket propulsion systems have been used for different missions.

Rocket propulsion systems provide the required energy for spacecraft to reach space, orbital maneuvers, or deep space explorations. Propulsion systems can be grouped by how they provide this required energy to the spacecraft or operation principle. These systems can be divided into three categories considering energy sources which are chemical, electric, and nuclear/thermal propulsion.

Propulsion systems provide a certain amount of momentum to the spacecraft with acquired thrust from the propulsion. This energy can be expressed by Newton's 2nd law, instantaneous spacecraft mass (m) and its velocity (u):

$$F = m\,\frac{du}{dt}$$

Thrust, a change in momentum, is provided from the ejected particles at a particular time ($\dot{m}$) from the nozzle with a certain nozzle exit velocity (V_e):

$$T = \dot{m} V_e$$

Propulsive thrust may change throughout the propulsion duration. Total impulse (I_t) is described as thrust force (F) integrated over a certain period of propulsion time (t):

$$I_t = \int_0^t F\,dt$$

Specific impulse (I_S) is described to characterize the propulsion energy sources. A higher specific impulse implies propulsion system produces higher thrust per unit mass. It is the total impulse per unit weight of the propellant.

$$A = \frac{\int_0^t F\ dt}{g_0\ \int_0^t \dot{m}\ dt}$$

To balance the equation g_0 is proposed as a constant 9.8066 m/s^2 standard acceleration of gravity at sea level on the earth. For a constant thrust and flow rate condition, this equation can be written as, a simplified equation where $\dot{m_p}$ defined as propellant mass flow rate:

$$I_s = \frac{F\ \ t}{m_p\ g_o}$$

These equations provide a basic understanding of the relation between the propellant and the target mission. The equation is also rewritten conveniently to relate it to the rocket's performance.

$$c = I_s\ g_0 = {}^{F}/_{\dot{m}} = \frac{p_1\ A_t}{\dot{m}}$$

Here effective characteristic velocity (c) is also defined as cee-star (c*). It is very handy because in a real system, exhaust velocity is not uniformly distributed through the nozzle; therefore, it is calculated as one-dimensional axial velocity.

$$V_e = c^*\ C_F$$

Exit velocity (V_e) can be related to characteristic velocity (c*) with the help of another characteristic parameter thrust coefficient shown as C_F. It comes from isentropic compressible flow equations from the nozzle.

The flow rate through an injector or a tube can be defined with the help of cross-sectional area, fluid density at the specific temperature, and the pressure difference between upstream and downstream. Here discharge coefficient (Cd) can be defined as the ratio of the actual flow rate to the theoretically expected flow rate.

$$\dot{m_{ox}} = C_d\ A \sqrt{2\ \rho_{fluid}\ \Delta P}$$

Time-averaged regression rate of solid fuel is calculated according to the initial and final port radius change throughout the burn time.

$$\bar{\dot{r}} = \frac{(D_{final} - D_{initial})}{2t_{burn}}$$

The oxidizer fuel flux also affects the regression rate of fuel. Oxidizer flux ($\overline{\dot{G_{ox}}}$) is defined as:

$$\overline{\dot{G_{ox}}} = \frac{16\dot{m_{ox}}}{\pi(D_{initial} + D_{final})^2}$$

Combustion efficiency ($\overline{\eta_{c^*}}$) is another parameter showing motor performance. It can be calculated as follows.

$$\overline{\eta_{c^*}} = \frac{P_c A_t C_d}{(\dot{m_{ox}} + \dot{m_{fuel}})c^*_{theo}}$$

Chapter 2:
CHEMICAL PROPULSION

Chemical propulsion systems generate thrust by the reaction of propellant and oxidizer through a chemical reaction. Heated and accelerated combustion products are ejected from a nozzle. These systems are commonly used in military, sub-orbital, launch vehicles, and space applications. Chemical propulsion systems can be mainly reviewed as solid, liquid, and hybrid propulsion systems.

2.1 Solid Propellant Motors

However, complex design components and storing the propellants in the liquid phase make liquid rocket engines expensive to test and develop. Also, many different toxic fuels/oxidizers are still used due to their high performance. The high performance comes with a high cost due to maintaining safety throughout storage and operation.

Monopropellant engines consist of a single propellant and a catalyst, or a heat source decomposes the propellant. In bipropellant engines, oxidizer and fuel react in a combustion chamber. These systems are very convenient because these engines have relatively simple in design with high specific impulse value. However, a lower thrust-to-weight ratio and relatively low limited control are the main disadvantages of these systems. Solid propellant rockets consist of an igniter and a fuel grain in which solid mixture of propellant and oxidizer are stored together. After ignition, the burning begins from the inner surface of the hollow solid propellant. Combustion products are heated and accelerated throughout the resilience time and ejected from a divergent-convergent nozzle. The main advantage of solid propellant engines is their simplicity. As oxidizer and fuel are stored together, any working fluid does not have to be transferred from a tank to a combustion chamber with complex designs such as pumps or valves. They provide high thrust-to-weight levels in proportion to their weight. Also, solid rocket motors can achieve specific impulses from 175 sec to up to 300 sec. However, the major drawback of the solid propellant motors is that safety caused by risk of explosion in storage and no chance to combustion termination after ignition.

2.2 Liquid Propellant Motors

Liquid propellant engines are a type of chemical propulsion system in that liquid fuel and oxidizer are stored in separate tanks. With the help of pressurization systems or turbopumps, the fluids are transferred to the combustion chamber. The main advantage of liquid propellant engines is that they provide flexibility to terminate the combustion. Also, with the help of fluid flow control elements, these engines can be throattable to obtain a specific thrust profile and reignited several times. Liquid rockets can provide specific impulses up to 400 sec.

2.3 Hybrid Propellant Motors

Hybrid propellant engines combine the beauty of solid and liquid-propellant engines. In hybrid rockets, the oxidizer and fuel are stored in different phases. Storage of fuel and oxidizer in separate phases and places increase the safety of the system. Generally, while the oxidizer is stored in the liquid-phase, the fuel is cast in a hollow cylindrical form and stored in solid form. A pressurized tank or turbopump feeds the oxidizer into the combustion chamber. The oxidizer can be throattable for some applications and can be re-ignited several times. Hybrid rockets can provide specific impulses up to 330 sec with some additives loaded to fuel grain.

Chapter 3:
PARAFFIN-BASED HYBRID ROCKETS COMBUSTION THEORY

Although the concept of a hybrid rocket has been around for nearly 85 years, it was not given considerable attention until the 1960s [1]. Conventional polymer-based hybrid rocket fuels are not the best options for high thrust level propulsion systems due to only the vaporization-driven nature promoted by heat transfer. Vaporization of fuel reduces heat transfer through the fuel grain, called the blocking effect causing a low regression rate [2]. The low regression rate issue may be overcome by modifying the flow field by changing injector design or inner grain geometry; however, scaling such rocket motors requires too much effort to unveil governing laws and correlation factors and correctly simulate heat and energy models. [2-3-4]

Paraffin-based hybrid rockets are demonstrated and, the governing art behind them is clarified by Karabeyoglu et al. as an alternative to conventional hybrid fuels [1]. Paraffin fuels show 3-4 times higher regression rates due to liquid layer instabilities promoted by liquifying, low viscosity, and low surface tension nature. Liquid droplets provide mass transfer from the liquid layer to the combustion chamber [1-2]. Mass transfer is driven from the unstable liquid layer to the oxidizer zone and burns as a spray with higher combustion surfaces by taking less energy for phase changing from the flame zone [5]. On the other hand, Paraffin-based hybrid rockets are mature and convenient candidates replace many conventional systems that have already operated in launch vehicles, upper stage, sub-orbital launch, micro/nanosatellites, and tactical missiles (including target drones) [6].

Chapter 4:
LITERATURE REVIEW

4.*1. Hybrid Rocket Fuel Grain Production Methods*

Different fuel manufacturing techniques can be preferred depending on the fuel blend character. Paraffin-based fuel propellants are generally manufactured by two methods which are direct casting and centrifugal casting. While the melt is poured into the mold and solidified with no external forces in direct casting, the blend is poured into a flanged tube and axially rotated at a specific angular velocity in the centrifugal fuel casting method. Paraffin waxes can shrink up to 15 to 20% while solidification [2]. With the help of centrifugal forces, these voids and bubbles are removed into the inner port and revealed.

The casting method and the process conditions quietly affect the grains' mechanical properties because the internal flaws cause the failures; therefore, process parameters highly affect the strength of the grains [7]. For large-scale fuel grain manufacturing, the centrifugal casting method requires more sophisticated and complex casting plants to ensure operational safety because huge amount of kinetic energy is stored in the rotating molds. Even though it provides mechanically more robust fuel grain, direct molding becomes the only option when energetic additives, including blends, are demanded. The reason behind this is the vast density difference between energetic additives and liquid paraffin matrix, causing phase separation due to centrifugal force. In the direct casting method, mechanically weakened or cracked fuel grains are generally obtained because air bubbles and voids are entrapped, and microcracks are formed while the blend solidifies. Somehow, both casting methods may not be the exact solution to obtain reliable fuel grain because space flight systems demand solid, cost-effective, and always operational components.

4.2 Hybrid Rocket Fuels in Literature

4.2.1 High Regression Rate Hybrid Rocket Fuels

Paraffin-based propellants are well-suited for a high regression rate required missions. In other words, the high thrust required application because a hydrodynamically instable liquid thin film layer under a high velocity gas flow provokes liquid mass transfer to the combustion zone,

which elevates the regression rate. The entertainment of the paraffin droplets is a function of fuel blend surface tension, melting temperature, and viscosity. The regression rate of the fuel can be rearranged by adding some additives, which also change the mechanical properties of the fuel. In literature, it is various studies have been conducted to improve the mechanical properties of paraffin-based fuels by either chemical or mechanical modifications. Effect of various thermoplastic additives such as ethylene EVA, LDPE, SEBS, SA, different tackifiers, and their mixtures have been analyzed by many researchers [8-9-10-11-12]. It should be noted that fuel mechanical property enhancement generally requires a trade-off with regression rate drop; therefore, these polymers should be diluted by paraffin wax for any high regression required application [13].

Efforts either to increase regression rate without trade-off from strength or to easy scale-up enabling techniques are investigated by different groups. Armold et al. conducted research that paraffin wax is directly poured into 3D-printed acrylic and machined for different port geometries and fired with axial and swirl injectors. Even though up to 270% increase in the regression rate is observed, some air bubbles around the 3D-printed structure are imaged by X-ray [12]. Bisin et al. printed 3D gyroid structures with different filaments and embedded into paraffin wax. The best performance is observed for ABS armored grain by 41% higher regression rate compared to neat paraffin. It is reported that the mechanical properties of the fuel grains are enhanced by embedded gyroid structure; however, heat deflection temperatures of the available filaments should be considered for large-scale grains [14]. Any manufactured fuel grain density data is not reported by either Armold et al. or Bisin et al, and all firing tests are conducted with comparatively lower combustion pressure than conventional high regression rate rockets. Furthermore, Pisciletti et al. conducted some research to prevent internal flaws propagation in neat paraffin wax fuel throughout the solidification process via heated circular mold under 10MPa pressure. The grains are separated two from their longitudinal axis, and the fracture surfaces are reported via microscopic images [14].

4.3 Low Regression Rate Paraffin-Based Liquified Hybrid Rocket Fuels

In hybrid rockets, low regression rate hybrid rocket fuel may be required for some applications such as upper-stage rocket motors, deep space explorations, etc. Thermochemical performance of fuel changes depending on the chemical structure and C, H, O ratio. Single bonded carbon-based backbone, no oxygen in the structure, and a higher H/C ratio are always desired for higher Is

values. High Is performance and low regression rate paraffin-based hybrid rocket fuel formulations may be developed by choosing high melting temperature paraffin waxes such as FT Waxes blends. Processing of such blends may be challenging due to the very brittle nature of the FT Waxes and thermal stresses caused by inhomogeneous cooling during solidification.

4.4 Hybrid Rocket Fuel Additives and Fillers

4.4.1 Polymer-Based Additives

EVA, SEBS, LDPE, SA, and PE, and tackifiers are the most used additives to enhance the mechanical properties of the paraffin-based hybrid rocket fuels. The mixtures should be carefully characterized because adding these additives affects not only the mechanical properties but also the rheological properties, which are critical parameters affecting the regression rate.

4.4.2 2D and 3D Fillers

Carbon nanotubes (CNTs), multi-walled carbon nanotubes (MWCNT), and graphene, polymer-based fibers are sometimes mixed with paraffin-based or polymer-based hybrid rocket propellants. While these additives can increase the mechanical properties of the fuel grain,depending on the addition ratio, they can positively or negatively affect the regression ratio of the grain. Chen et al. worked to enhance the combustion properties of the HTPB fuel with some additives and innovative methods. It is observed that 1% addition of MWCNTs to HTPB-based fuel grain increases the regression of the grain by about 31.6% [16].

4.3.3 Energetic Additives

The primary motivation behind adding metal additives to fuel grains is the enhancement of specific impulse, density impulse, or regression rate. Additive material selection is made by considering different aspects such as performance effect, availability, cost, lifetime of fuel grain, ballistic effects, and environmental impact. Cost and availability are the primary drivers of material selection for commercial applications. These energetic additives do not significantly enhance high-performance oxidizer-selected fuel and oxidizer duos. In contrast, for low-energy oxidizer duos, the addition of energetic additives improves the propulsive performance [17]. The performance enhancement can be obtained with some mechanisms such

as improvement of combustion heat, or adiabatic flame temperature, significant regression rate or Isp increase. Aluminum-based powders deliver reasonable Isp performance improvements at a plausible price.

As these formulations cannot be cast by the centrifugal casting method due to the high-density difference between the paraffin wax blend and energetic metal additives, the grains should be processed by the direct pouring method. These grains are prone to fail during direct pouring because high viscosity triggers air bubble entrapment and crack formation in solidification.

Mostly used energetic additives are lithium-based (Li), aluminum-based (Al), magnesium-based (Mg), lithium-aluminum-hydride ($LiAlH_4$), and ammonia-borane (BH_3NH_3). Lithium is one of the energetic additives which shows high reactivity. Boron-based particles' main advantage is high combustion energy acquisition per unit mass, but it is resistant to ignition. In commercial applications, aluminum is one of the most appropriate additives due to its lower cost than other energetic additives and significant specific impulse improvement without compromise from practicality.

The particle size of the additives and how well it is processed with binder fuel are also important. The regression-rate of liquified fuels is increased by decreasing fuel melt viscosity. Using smaller particle size increases the viscosity and tendency to agglomerations. These agglomerations behave as stress concentration points in the grain and negatively affect the fuel grain's mechanical properties.

These agglomerations may also cause low-frequency combustion stabilities due to diffusion and thermal feedback to the grain. Furthermore, the thrust generation may be lost in time due to unburntmetal agglomeration on the surface. [17].

4.3.*4 Hypergolic Additives*

Hypergolic additives can provide spontaneous ignition. Jobin et al. conducted a research to investigate the ignition delay and the mechanism behind it by working with paraffin & hypergolic metal-organic frameworks (HMOFs) fuel mixture with white fuming nitric acid [18]. Rang et al. investigated the reactivity of different binder & hypergolic additives combined with industrial-grade hydrogen peroxide. They conclude that PW binder exhibited effective burning with low activation energy and strong flame compared to HDPE. Due to mechanical strength limitations and liquefied nature, they decided to work with HDPE [19]. Also, Carayon et al. conducted research to develop paraffin-based hypergolic grain. They manufactured two-inch outer, one-inch inner, 9-inch length fuel grain doped with sodium

amide up to 90% in some sections and ignited with MON-3 oxidizer. They concluded that using a higher percentage of hypergolic additives makes the direct casting process harder [20]. Hypergolic hybrid rocket fuel manufacturing and ignition delays are investigated on pellet-droplet scale or small-scale motors. For future studies, homogenously manufactured fuel grain may be requested.

Obviously, a consistent paraffin-based large-scale energetic additive, including fuel formulation casting, is a challenging process. A new method enabling grain manufacture at any scale, no matter if the fuel formulation contains energetic additives or not, is demanded for many applications.

In this article, a new approach, paraffin-based hybrid rocket fuel sintering, is introduced. Fine powders in different formulations are fabricated with different techniques, then sintered in a cylindrical mold under pressure and temperature. These grains' mechanical properties are compared with those of centrifugally cast ones. The parameters affecting the mechanical properties and the mechanism behind them is discussed with some characterization methods.

Chapter 5:
DEVELOPMENT OF NOVEL PARAFFIN BASED HYBRID ROCKET FUEL PRODUCTION METHOD

5.1 Materials

Paraffin wax, FR5560 was purchased from Candlewic and ethylene vinyl acetate (EVA), Escrone Ultra UL 40028 was purchased from Exxonmobil. As an energetic additive, aluminum powder having 3-micron size and 98.75% purity was purchased from Nanomaterial Powder Company from Turkey. Sylvares 6100, styrenated-terpene produced by Kraton was supplied from Sar Chemical, Turkey. 99.9% purity isopropyl alcohol was purchased from Turkey. Also, KWC DYE 366 black is purchased from Kaiser Turkey. Metallic additive 3 microns aluminum powder is supplied from Nanokar, Turkey. As blowing agent JoySun W3835 is provided from Joysun.

5.2 Powder Manufacturing Methods

Neat paraffin wax blocks are melted in a 40-liter melting pot, then thermoplastic additives are blended with the melt by high-shear mixer for 1hr. After mixing, it is processed to obtain powder by desired manufacturing method.

5.2.1 Blend Quenching Method

In this method, for manufacturing fine powder, liquid paraffin blend at 90°C and isopropyl alcohol (IPA) at room temperature are prepared in different pots. Then, as soon as a small amount of paraffin blend is poured into IPA pot, it is granulated by mixing to gather coarse granules. The granules are spread out on a filter to drain out for 24hrs. After the excess isopropyl alcohol is vaporized, the granules are put into a 25-liter ball-mill with 10mm stainless steel balls and break into fine particles. After 6hrs of ball-milling, it is transferred into a meshed sieve to clean out the fine particles from excess unfragmented granules and metal balls. The powder is sieved one more time into the sieve to ensure the maximum size of the particles in the fine powder.

5.2.2 Powder Atomization Method

Another novel paraffin powder production method was introduced to make possible, easy, and mass production for large-scale fabrication.

Powder atomization is the primary method to obtain ceramic and metal powders. In this method, the molten material is fed through a nozzle via a pipeline from the melting pot. Depending on the application method, the molten material is separated into micron-sized droplets by high-energy jets of a liquid. The spraying system is specifically designed to obtain desired particle size and shape.

For this application, the paraffin blend is atomized by a specially designed nozzle fed by a gravity-driven, 40-liter heated tank. Throughout the process, as a jet, high-purity gas nitrogen is used to atomize to inhibit any contamination and oxidation. The atomization occurs in a 600 mm in diameter silo to gather fine particles. Figure 5.1 illustrates the designed system to manufacture fine paraffin powder.

When blend quenching and atomization methods are compared, powder atomization requires less effort compared to the blend quenching method. Also, for specified systems, while the blend quenching method makes it possible to manufacture paraffin blend 1kg/day, powder atomization allows to manufacture up to 150kg/day.

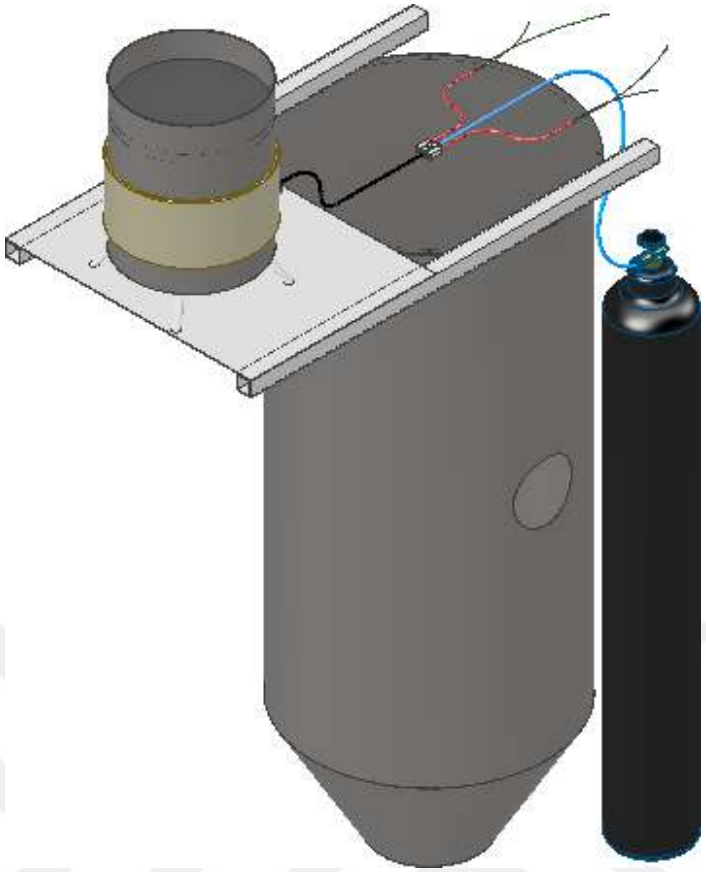

Figure 5.1 40-liter heating and mixing tank with atomization reactor and gas source.

5.3 Fuel Grain Manufacturing Methods

5.3.1 Cold Compression Method

Powders are compressed in 110mm outer, 30mm inner diameter, 200mm length, cylindrical mold. The mold is heated both from outside, wrapped rope-type heaters and, from the inner rod, drilled and placed cartridge-type heater having K-type thermocouples. The design can be seen in Figure 5.2. It is gradually compressed under a 15-ton-weight capacity hydraulic press automated with PLC controller.

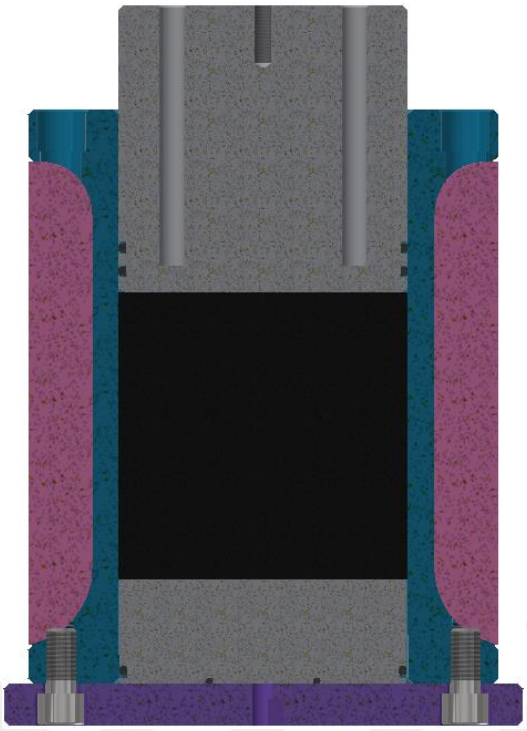

Figure 5.2 Final mold designed to investigate mechanical properties and process parameters.

5.3.2 Hot Compression Method

If the desired fuel formula has no higher density additives, it is directly added to the mold. Otherwise, it is mechanically mixed with the additives within a 20-liters screw mixer designed for and manufactured for this project. The design can be seen in Figure 5.3. After the powder preparation, the mold is heated to the assigned temperature, and powder material is added. The mold is processed under the hydraulic press at a specific temperature and pressure.

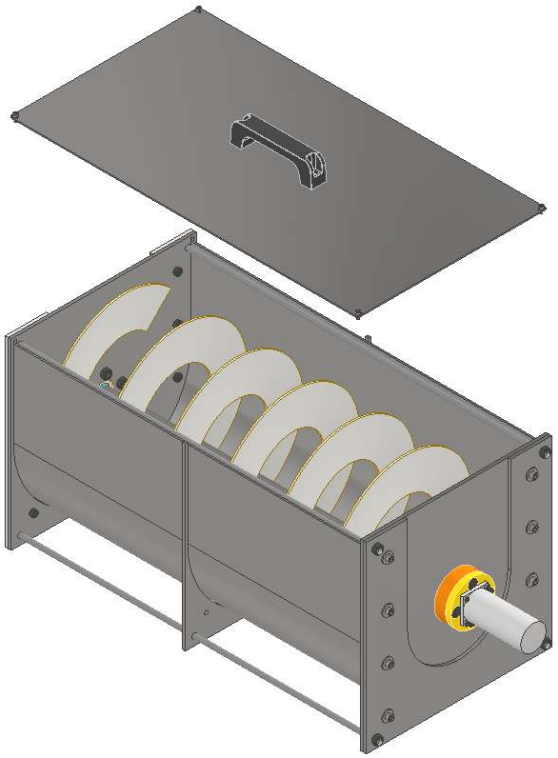

Figure 5.3 Screw mixer design to mix paraffinic fuel powder with additives.

5.4 Characterization Methods

5.4.1 Optical Microscope

Powder shapes and sizes are visualized and captured with Metkon IMM 902 optical microscope Mshot MS60 microscope camera apparatus. The visuals are post-processed with ImageJ to measure the average particle size.

5.4.2 Density Measurement

The density of compressed and sintered grains is measured by Archimedes' principle in 99.9% purity isopropyl alcohol.

5.4.3 Mechanical Testing

Mechanical properties are investigated by tension test method. Manufactured grains are machined by milling and lathe operations to get cylindrical dog-bone specimens in 8 mm gage width, 30 mm gage length, and 10 mm radius. Tension tests are performed with 2mm/min

crosshead displacement by a 1kN Shimadzu AGS-X universal testing machine. First, each specimen is preloaded to1N to be sure that the specimen is axially loaded, the test is conducted. Then, the data is post processed to get rid of the garbage data up to actual loading.

5.4.4 Thermal Analyzes

DSC analyses are performed with TA Instruments, DSC25 model. Degree of crystallinity and thermal history of the fabricated powders and fuel grains areanalyzed with closed pans and non-isothermal mode. Crystallization and melting behaviors of the materials are investigated.

5.4.5 Scanning-Electron Microscope

Tension specimen fracture surfaces are investigated by LEO Supra VP35 fieldemission scanning microscope after sputter deposition of a thin conductive Au/Pd coating of the samples.

5.4.6 Structural and Thermal Analyzes

Paraffin wax is a sensitive material due to its low strength and poor strain capacity. Heating and cooling cycles around its solid-solid phase transition or processing near its melting temperature can cause microcracks. Therefore, it should be handled carefully during processing, especially when sintering. After conducting some sintering experiments, it was observed that the fuel grain is prone to cracking when processed in the first mold configuration, as shown in Figure 11.4.
Some end capping and directional flow patterns into the centerline of the fuel grain were observed at the crack surfaces. As a result, the solidification process of the paraffin blend under a certain pressure was simulated using Ansys steady-state thermal analysis. The fuel formula is defined in the engineering data. The density at ambient conditions is specified as 928 kg/m³, as given in the new paraffin wax datasheet. Tensile and compressive properties are defined according to previously characterized material mechanic tests. Thermal conductivity and specific heat are set to 0.21 W/mK and 2100 J/kgK, respectively. The melting temperature is defined as 68°C, as observed from DSC isothermal scans.
Program-controlled heating boundary conditions are defined for heater contact surfaces. The film coefficient and ambient temperature for these surfaces are specified as 0.1 W/mm²°C and 67°C,

respectively. Except for these surfaces, each surface is described as a convection surface. One million quadratic elements are aimed for each run, and seven different mold combinations are evaluated.

In Figure 11.4, Configuration 1 was the initial geometric combination used to produce the first fuel grains through cold compression, and no crack propagation was observed during this manufacturing process. However, when the mold was heated for sintering process experiments, crack formation was observed at the beginning and the end of the grain in many specimens. Even the ones manufactured without cracking later came apart during specimen machining. It is observed that cracking surfaces overlap with the temperature distribution of configuration 1. Vast density change around melting temperature creates too much volumetric change throughout hot compression process. Also, inhomogeneous heat distribution cause uneven cooling and tend to crack into chunk parts; therefore, temperature distribution at the steady-state should be minimize as much as possible.

Most crack formations were specifically observed at the surface close to the top surface, with some crack surfaces being smooth and parallel to the top and end surfaces. It was understood that after the mold was fully filled, the powder was compressed with more force than required, making it difficult for the added powder to weld to the contact surface, resulting in apertures.

To address these issues, a flanged tube was introduced in the design Figure 11.5 to provide extra volume for filling the mold during the initial powder addition and compaction. Although these revisions improved the consistency of the process and specimen machining, the cracking problem persisted after sintering. Further revisions were discussed in Figure 11.6, including heating the inner rod, and compressing with a more appropriate piston.

Even though directional flow patterns were observed at the crack surfaces, high densities were still achieved. This led to the belief that inhomogeneous cooling played a role in enhancing crack formation. Therefore, some revisions were made to the piston and mold, such as placing four heating cartridges into the piston and isolating the mold with fire-resistant insulation foam. The effects of these additions were analyzed, and the results are presented in Figures 11.7, 11.8, and 11.9.

Despite these revisions, some heat gradient was still observed under the fuel grain in Ansys analysis. As a final iteration, the bottom sealing plate was thickened (Figure 11.10). This modification significantly reduced the maximum temperature difference from 13°C in the initial configuration to less than 0.5°C in the final version. Although some minimal gradient was observed at the bottom of the fuel grain in the first 5 mm, it was deemed insignificant for specimen production. Upon investigating the crack surfaces, no flow direction was observed. For detailed information on each configuration, refer to Table 5.1.

Table 5.1 Ansys Model Configurations.

Configuration	**Mold Insulation**	**Inner Rod**	**Bottom Sealing Plate**	**Upper Sealing Plate**	**Piston**	**Accessory**
Configuration 1	☒	☒	☑ 8mm	☑ 8mm	☑	☑ Block
Configuration 2	☒	☒	☑ 8mm	☑ 8mm	☑	☑ Extension
Configuration 3	☒	☑ With Heater	☑ 8mm	☑ 8mm	☑	☑ Extension2
Configuration 4	☒	☒	☑ 8mm	☑ 8mm	☑ With Heater	☑
Configuration 5	☑	☒	☑ 8mm	☑ 8mm	☑	☒
Configuration 6	☑	☒	☑ 8mm	☑ 8mm	☑ With Heater	☑
Configuration 7	☑	☒	☑ 40mm	☑ 8mm	☑ With Heater	☑

5.5 Results

Two different formulas were defined to manufacture fuel grains to conduct some mechanical tests. It was observed that pressure, temperature, and heating time play an important role in the mechanical properties of a fuel grain; therefore, the effect of processing parameters were investigated using specimens taken from the fuel grains processed with different pressure, temperature, and heating time. Many different fuel formulations have been proposed in the literature, and EVA, one of the most common paraffin additives, was chosen to formulate a paraffin-based fuel grain. According to some preliminary tests, the 2% named as P/2EVA and 10% EVA named P/10EVA added fuel formulas were preferred to focus on. 0.5% dye was added to paint black for fire tests. The DSC graphs of neat paraffin wax, EVA, and the P/2EVA fuel formula are given in Figure 5.4

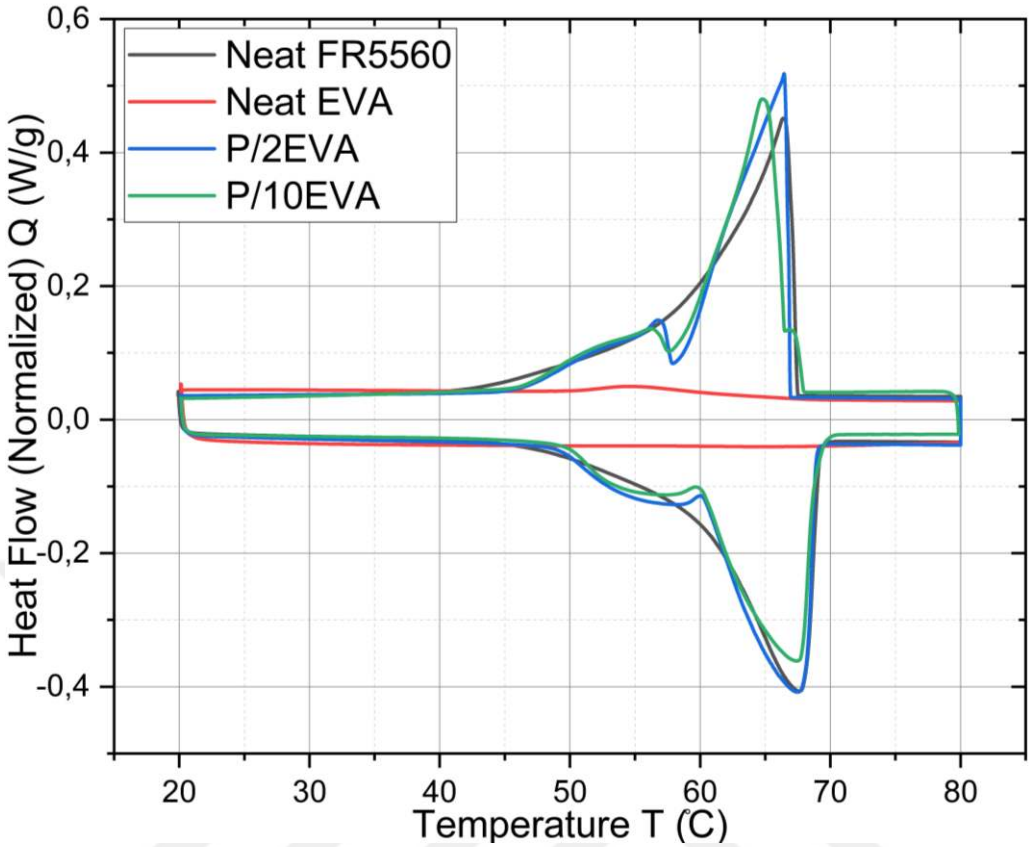

Figure 5.4 DSC Result of neat materials and formulations

Both formulations can be defined as crystalline due to high degree of crystallinity calculated by the equation given below.

$$X_C = \frac{\Delta H_f(T_m)}{\Delta H_f^{\circ}(T_m^{\circ})}$$

It is observed that P/2EVA and neat paraffin wax show similar exothermic peaks. On the other hand, P/10EVA displays an earlier peak formation than expected neat paraffin wax main crystallization peak. It indicates that different phase formation may occur during solidification, or higher percent EVA addition restricts mobility of paraffin wax chains.

Mechanical properties of centrifugally casted fuel grains are investigated by the mechanical tests done to the specimen machined from 110mm outer diameter, and 30mm inner diameter fuel grains. The results are shown in Figure 5.5. It is observed that while P/2EVA formulation show 3.7MPa tensile strength and 2.55% strain capability, P/10EVA formulation shows 3.3MPa tensile strength and 5.1% strain capability. It is well-known that process parameters affect the centrifugally casted fuel grain's mechanical properties. Inappropriate casting temperatures, cooling rates, insufficient centrifugal force may cause some micro defects and low degree of

crystallization. Throughout the research, while the crack formations are examined by eye inspection, micro defects are investigated by density measurements with Archimedes' principle. Moreover, thermal history and the degree of crystallization is measured by DSC analysis. Results are given in Table 5.2.

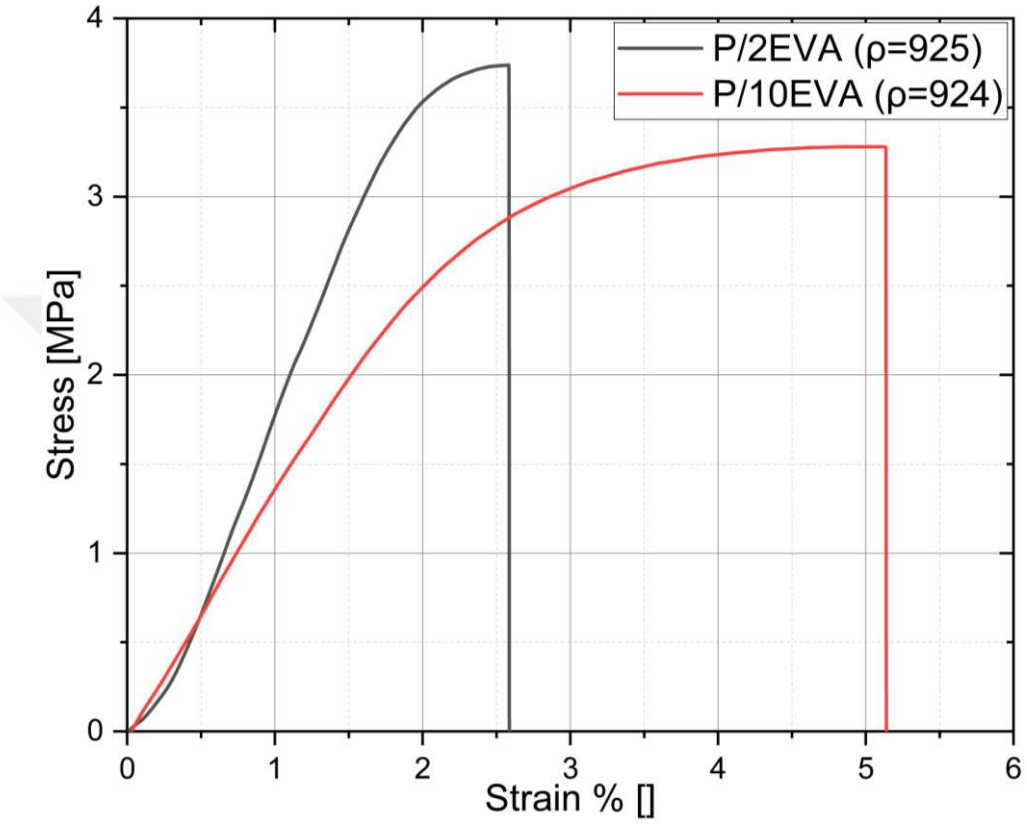

Figure 5.5 Centrifugally Casted Fuel Grain's Tension Test Results

Table 5.2 Properties of fuels manufactured by centrifugal casting.

Formulation	Manufacturing Method	Tensile Stress [MPa]	Tensile Strain %[]	Relative Density kg/m^3	Degree of crystallinity %[]
P/2EVA	CC*	3.7	2.55	0.996	98
P/10EVA	CC*	3.3	5.1	0.994	99

CC*: Centrifugal Casting.

Both grains have high relative densities, and the degree of crystallization is very close to theoretical results with 98% and 99% degree of crystallinity for P/2EVA and P/10EVA respectively. It is observed that centrifugal casting is properly performed for P/2EVA and

P/10EVA formulations.

P/2EVA and P/10EVA powders are manufactured by atomization method to use in powder characterization, and fuel grain manufacturing. It is well known that powder particle size, shape, and porosity play an important role for powder metallurgy. Low particle size provides larger surface areas to interact with neighboring particle for bonding and higher packing density throughout the process. Also, irregular shaped particles tend to interlock with each other and increase the trans-granular crack path. For metal sintering, porosities may decrease the final density of the bulk material, the porosity of the paraffin-blend powder is not investigated in this research. After atomization, the powder undergoes a 300 microns metal sieve to prevent from undesired junk particles. The SEM images taken from P/2EVA, P/10EVA blends are given in Figure 5.6. As can be seen, all particles have spherical shapes and have different size. Relatively low viscosity, and surface tension let the liquid droplet reach to spherical shape which is the lowest energy state. Also, it is observed that 90% of the particles are smaller than 15 microns with help of MATLAB image processing tool. The effect of particle size and distribution among the powders produced from different batches is ignored for this research.

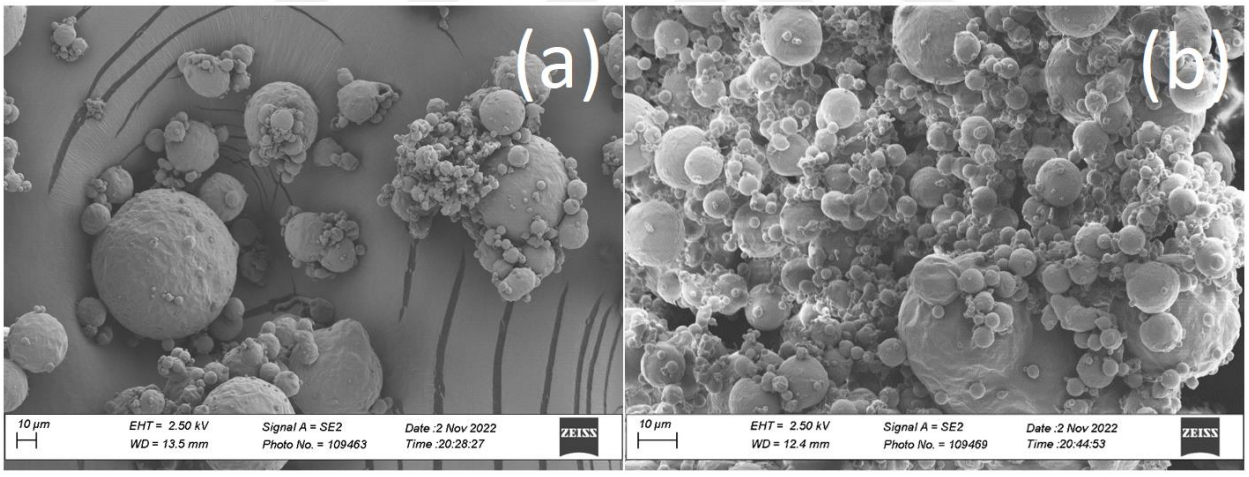

Figure 5.6 SEM imagining of atomized (a) P/2EVA added and (b) P/10EVA added formulations.

P/2EVA formulation powder is filled into the mold and compressed under different pressures for 5 minutes to investigate the effect of pressure on the bulk density of fuel grains. It is observed that all grains showed higher than 99% relative density (over 920 kg/m^3) over 3.5 MPa compaction pressure. While the increase of compaction pressure highly increases the density up to 4.5 MPa, the effect of increasing the pressure slightly diminishes. Compression tests on P/2EVA and P/10EVA formulations are performed to understand the relationship between the compaction pressure and mechanical properties of the powder which is going to be handled. The results show that performing cold compression slightly over the ultimate compression strength is enough to

obtain a similar relative density to centrifugally cast fuel grains. Additionally, it should be noted that the surface quality of the moving parts and the friction between the piston and the mold affect the load transfer between the piston and the powder.

Some tension test specimens are machined from the cold-compressed fuel grain processed between 3 MPa to 6 MPa for 4 different scenarios. All cold compression cases display brittle fracture without any plastic behavior. Even though high relative density is an indicator of an insignificant amount of void formation, defects at any scale cause mechanical performance loss. Independent of EVA concentration, similar tensile strength and strain capability indicate that the fracture takes place before EVA molecules show any elongation or reptation. Polymer-based green compact materials generally display low mechanical strength compared to their melt-processed version due to a lack of physical welding of granules to each other.

The micro-scale aspect of the problem is examined by SEM visualization of the fracture surface of the test specimens taken from centrifugally cast and taken from cold-compressed fuel grain. The fracture surfaces can be seen in Figure 5.7. While the centrifugally casted specimen experienced intergranular fracture, the spherical marks on the cold-compressed specimen's fracture surface verify the inter-granular fracture before any plastic behavior. It proves that even though slight tensile strength enhancement is attained by increasing compression pressure, the lack of interparticle bonding causes early fracture before any plastic behavior.

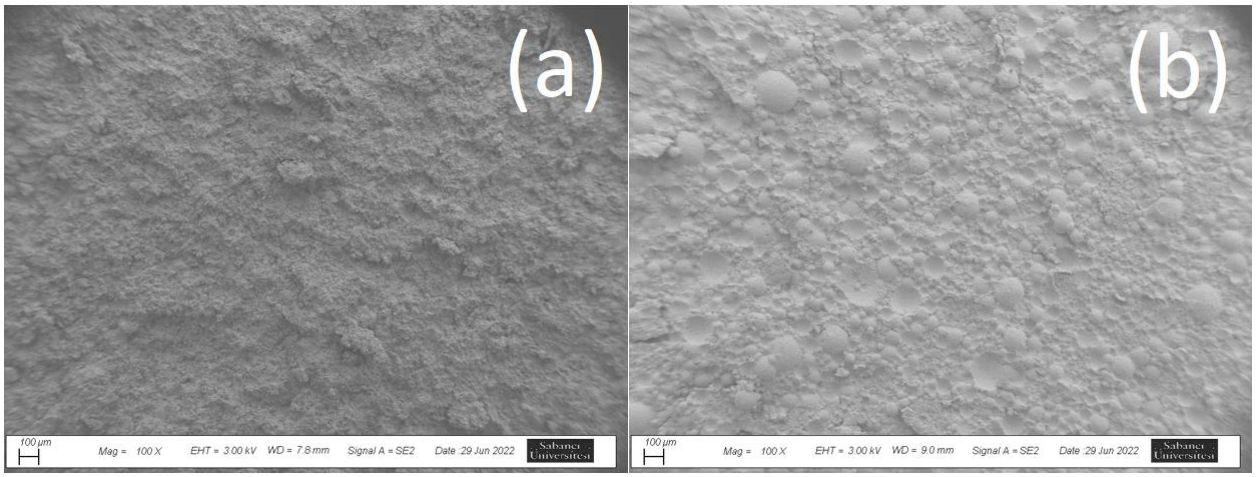

Figure 5.7 SEM imagining of specimen machined from (a) centrifugally casted and (b) cold compressed fuel grains.

Thermal history and the degree of crystallinity play a crucial role in the mechanical properties, especially for highly crystalline materials like the low concentration thermoplastic alloyed paraffin wax blend used in this study. DSC analyses are conducted on the samples taken from beneath the fracture surface of the cold-compressed specimen. Additionally, a 30-gram sample

is taken from atomized powder and manually mixed in a container to ensure homogeneity. The DSC analyses are performed both after one day and after 30 days. The powder's degree of crystallinity after atomization is found to be 92%. The cold compression samples show the same degree of crystallinity as the atomized powder. According to the literature, the degree of crystallinity of a polymer can only be tailored by gigapascal-level pressures; therefore, the crystallinity of the cold compression samples confirms the crystallinity of the powder samples. After one month, the degree of crystallinity of the sample taken from atomized powder is measured as 99%. This result indicates stress relief in the powder that occurs at room temperature over a month. The crystallinity result of 92% is significantly lower than the expected and reported values in the literature.

During the atomization process, the melt is fed above the melting temperature and atomized by the gas at room temperature. The abrupt solidification within milliseconds causes a flash cooling effect, which slightly inhibits the mobility of paraffin chains. As a result, the atomized powder shows a lower degree of crystallinity until stress relief happens at room temperature in a couple of days. To support this argument, the degree of crystallinity of a neat paraffin wax sample is examined by DSC analyses with different cooling rates ranging from 5°C/min to 60°C/min. It is observed that the cooling rate does not have any effect on the degree of crystallinity up to 60°C/min. The mentioned cooling rates are still well under the cooling rate expected during the atomization process. Further investigation should be conducted with a flush DSC to analyze the fuel blend with high cooling rates like 500-1000°C/sec.

Hot compaction and pressureless sintering are two main methods to obtain polymer-based parts. In thermodynamic aspects, the system goes into a relatively more thermodynamically stable state while decreasing its Gibbs free energy throughout sintering. The small particles come together and, due to coalescence, bigger and lower surface free energy particles are formed. Coalescence enhances the mobility of the polymer chains and the rate of diffusion. Depending on the polymer characteristics, such as chain structure, molecular weight, and processing parameters, mechanical properties are improved. Increasing compression pressure and temperature positively affect the diffusion kinetics. The sintering temperature is determined depending on the material's melting and crystallization temperatures. The super-cooling window is a temperature region in which the material is in a supercooled state, meaning it is in a liquid state below its solidification temperature. The representative graph can be seen in Figure 5.8. The forementioned temperature gap, super-cooling window, is not observed for paraffin waxes with such small length and homogenous similar chains. The window is also not observed for P/2EVA and P/10EVA formulations.

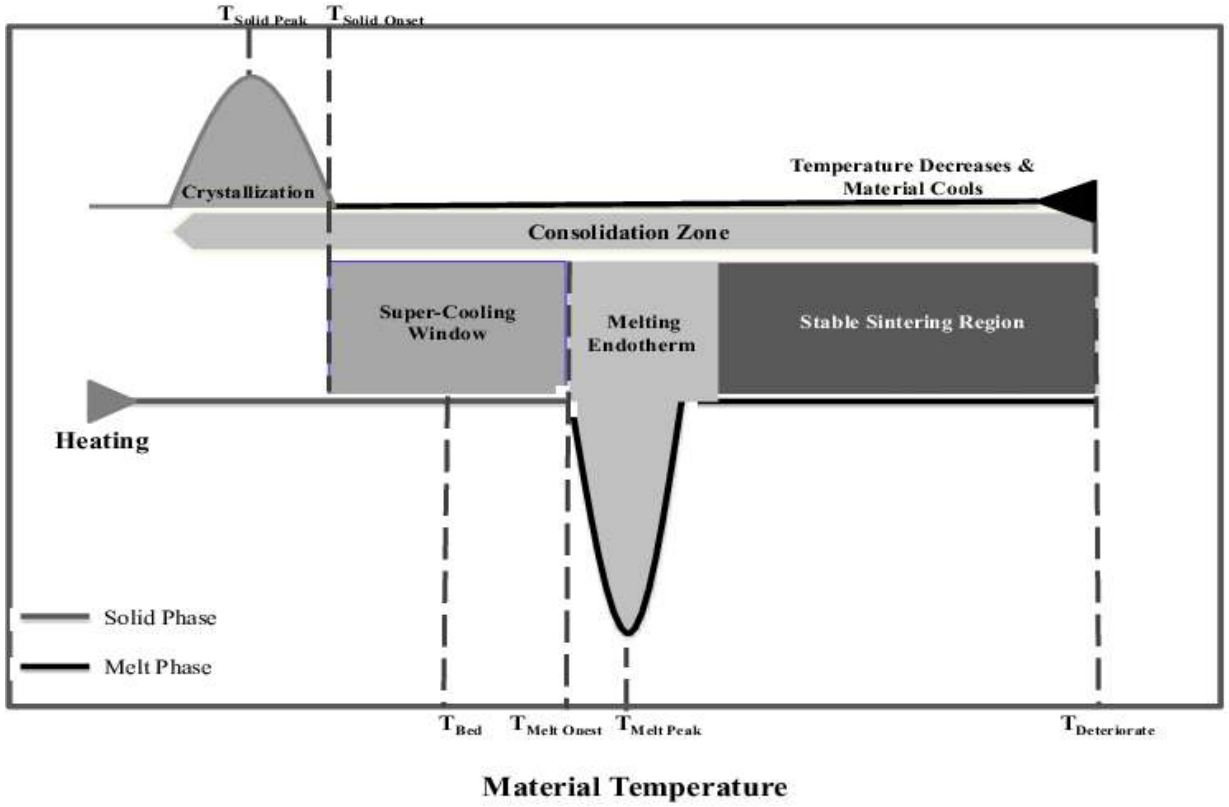

Figure 5.8 Super-cooling window shown in a DSC analysis.

To evaluate an alternative aspect, pressureless sintering is applied to cold-compressed fuel grains. The powders are compressed under 6MPa compaction pressure at room temperature, and then these grains are placed into an oven heated with infrared light. The temperature of the grains is monitored from the surface of one of the grains by a probe. The temperature is actively controlled by a PID controller. The grains are heated to 55°C, 60°C, 65°C, and 67°C for 24, 48, 72, and 96 hours. After the grains are taken out, a sponge-like structure is easily observed by eye inspection for the grains heated to 65°C and 67°C. The experiment is repeated for these cases, but any specimen cannot be machined from the fuel grains heated to 65°C and 67°C temperature. Any notable mechanical enhancement is not obtained from the performed tension tests processed at 55°C temperature. Notable mechanical enhancement is only observed for 60°C heated specimens; however, notable mechanical property enhancements are not attained depending on the heating time. The fracture surface of the specimen exposed to 60°C for 24, 72, and 96 hours is scanned by SEM. The surfaces can be seen in Figure 5.9.

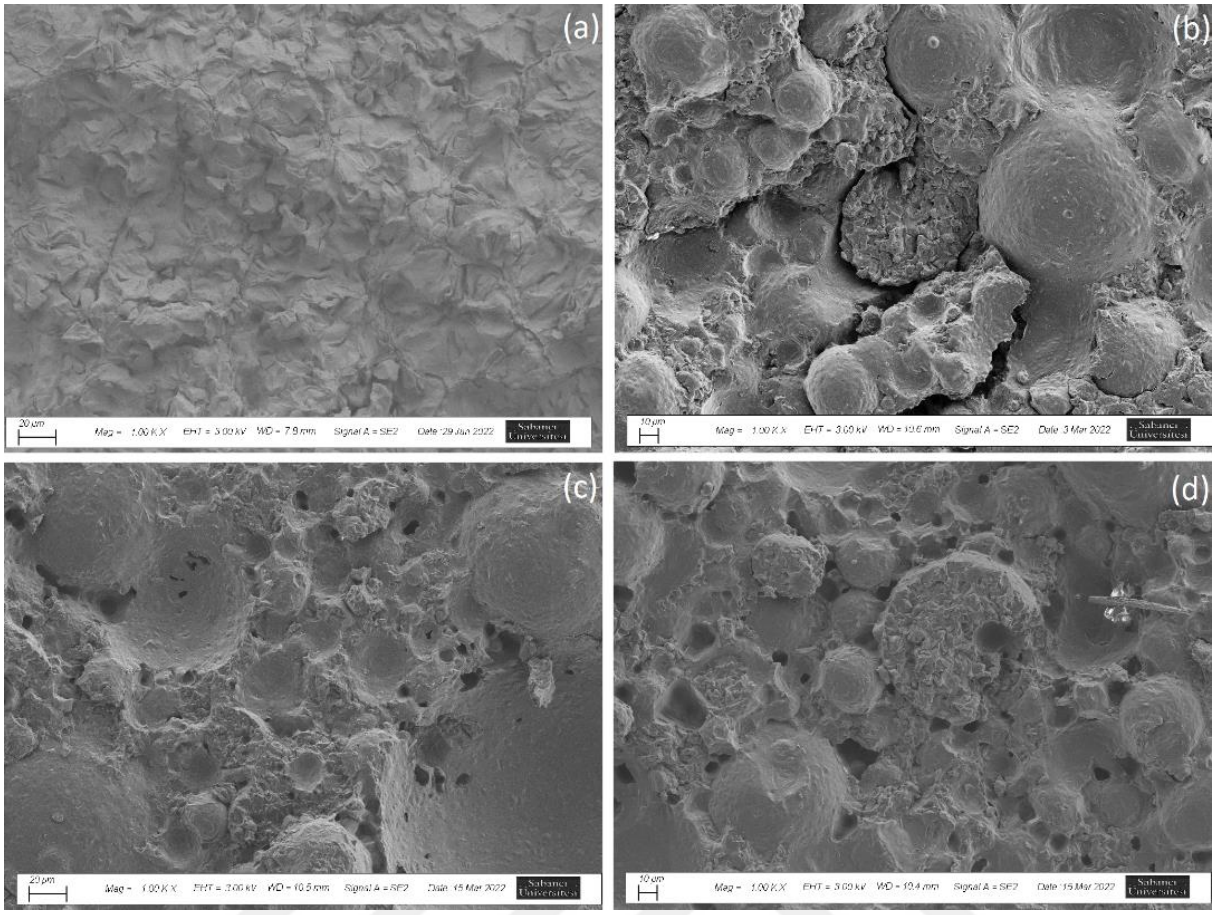

Figure 5.9 Fracture surface of (a) centrifugally casted, pressureless sintered fuel grains at (b) 60C for 24hrs, (c) 60C for 72 hours, (d) 60C for 92 hours.

Compared to the cold-compression specimen's fracture surface, trans-particle crack formation is achieved because of pressureless sintering. As expected, particles have bonded to each other at the contact surfaces; however, break apart from neighboring particles without any plastic deformation is still observed for some particles. Also, voids are clearly observed among the powder granules and the inner parts of these granules. It is measured that after the pressureless sintering process, the density of the specimens is significantly decreased from 922 kg/m^3 to around 850 kg/m^3. The reason behind these decreases is the density variation of the paraffin-blend depending on the temperature. The solid-solid phase transition is observed after 49°C from the DSC analyses. It indicates that above this temperature, density decreases, and the grain remarkably expands; then the decrease in temperature causes void formation. The tensile strength of the manufactured grain is decreased from 2.4 MPa to 1.9 MPa with no change in strain capability. The tension test results of each case can be seen in Figure 5.10. Even though trans-granular fracture, which can be seen in the fracture surfaces, is attained for many particles at the fracture surface, micro-void formation and density decrease eliminate the expected mechanical property enhancement. Results indicated that in the case of micro-void-free heat treatment, an enhancement in the mechanical properties of the fuel grains can be achieved.

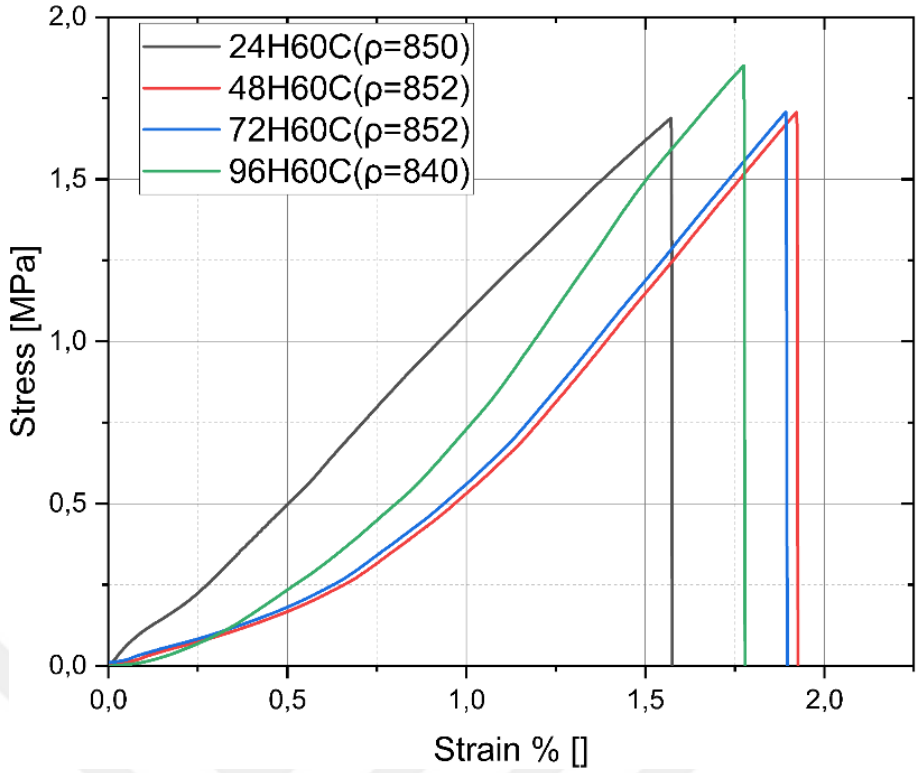

Figure 5.10 Pressureless sintered P/2EVA specimen's tension test results.

Hot compaction is another method applied to fuel grains to investigate the effects on the fuel grain mechanical properties. In this method, the cold compression mold is heated as mentioned in the above configuration. The mold is preheated to the process temperature, and the powder is added to the mold and compacted under a certain pressure. It is observed that mold design, pressure, temperature, time, and cooling rate play a crucial role in the mechanical properties and the unity of the fuel grain. Experiments for P/2EVA and P/10EVA are conducted at different times and temperatures for 6MPa compaction pressure. While processing powder at a higher temperature than room temperature decreases the ultimate and yield strength, which makes 6 MPa compaction pressure suitable. Many samples are manufactured at 60°C, 65°C, and 67°C for 12 hours, 24 hours, and 48 hours. As some fuel grains are cracked while demolding or machining, the same fuel grain is processed under the same conditions many times. A threshold temperature and time profile are observed to achieve an improvement in mechanical properties. Heating for less than 24 hours at a temperature lower than the melting temperature causes cracking during the machining process for any fuel formulation.

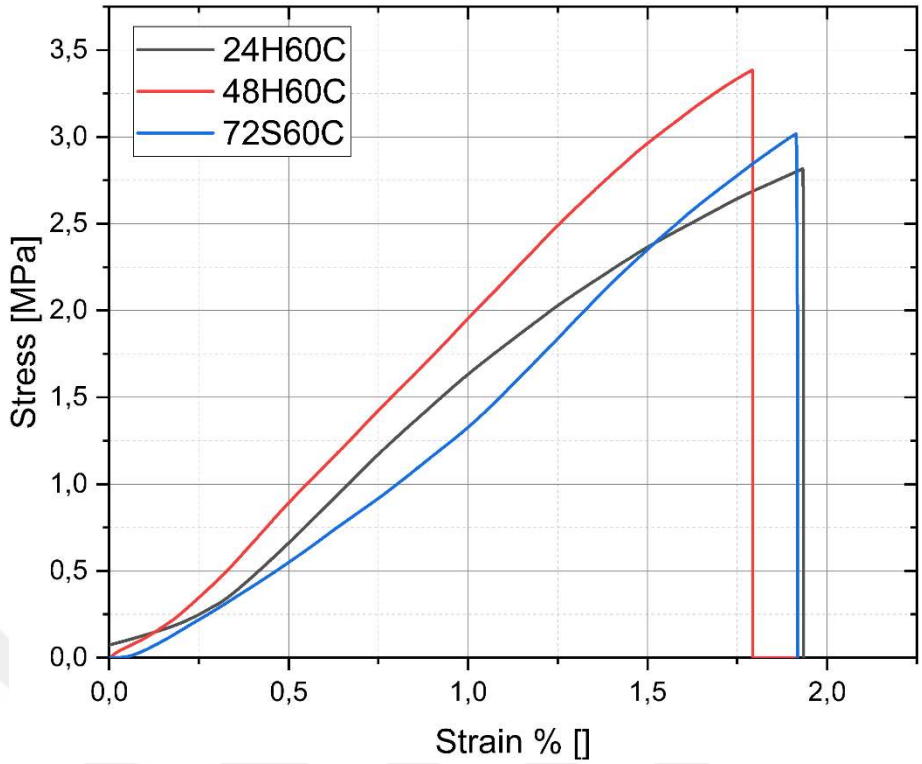

Figure 5.11 P/2EVA Formulation Hot Compaction Tension Test Results

Moreover, to investigate the effect of processing temperature, P/10EVA powder is sintered at 60°C, 65°C, 67°C, 68°C, and 70°C temperatures. The results can be seen in Table 5.3. It is observed that changing the process temperature does not result in any significant mechanical property change; however, even though a couple of attempts were made to sinter P/10EVA fuel grain at temperatures higher than 67°C, any solid fuel grain was not successfully manufactured. As can be seen in Figure 5.11, at around 68°C, the fuel formulations display an endothermic peak which implies that most of the volumetric change is observed around this temperature. Even though the fuel displays viscoelastic properties at these temperatures, the temperature gradient under pressure causes micro-cracks and directional flowing.

Table 5.3 Tensile properties of P/10EVA fuel grains sintered at different conditions.

Formulation	Processing Time (Hours)	Processing Temperature (°C)	Tensile Strength [MPa]	Tensile Strain % [ ]
P/10EVA	24	60	2.8	1.8
P/10EVA	24	65	3.2	1.9
P/10EVA	24	67	2.6	1.8
P/10EVA	24	68	-	-
P/10EVA	24	70	-	-

Some other parameters that have been ignored in their effects may also be carefully investigated. Additionally, the effect of some 2D and 3D fillers should be demonstrated. Lastly, the solidification process parameters should be carefully investigated, like how the mold heating conditions were examined.

Further tests with 0.25%, 0.5%, and 1% CNT addition to the P/2EVA formulation and the mechanical properties of sintered P/2EVA and P/10EVA fuel grains are conducted at the same processing conditions. After many sintering tests, it is observed that 24 hours of sintering at 65°C generally result in consistent uncracked, and no leak observed fuel grains. Therefore, the tests that are going to be conducted are planned at these sintering conditions.

After preparing the paraffinic fuel melt, CNT is added to the melt and mixed with high shear for 4 hours at a temperature between 70-80°C to prevent any agglomeration. Then, the mixture is placed into an atomization system at the minimum quantity while the melt is kept mixing with high shear. Some compression tests are conducted on P/2EVA and P/10EVA specimens machined from centrifugally casted fuel grains. The results are compared with the ones manufactured by the sintering method. Additionally, some compression specimens can be machined from CNT added fuel grains. The results can be seen in Table 5.4.

Table 5.4 Compression Test Results.

Formulation	Compressive Strength [MPa]	Comressive Strain % []	Compressive Modulus [MPa]	Density kg/m^3
P/2EVA_CC	3.5	3.25	150	918
P/10EVA_CC	3.9	3.25	167	915
P/2EVA_S	3.5	3.1	155	920
P/10EVA_S	3.8	5.9	170	921
P/2EVA/0.25CNT_S	4.1	3	200	919
P/2EVA/0.5CNT_S	3.8	3.3	250	920
P/2EVA/0.1CNT_S	3.8	3.7	200	919

CC: Centrifugally casted, S: Sintered,

It is observed that both centrifugally cast and sintered specimens for the P/2EVA and P/10EVA formulations show similar compressive properties. An increase in the compressive strain for the sintered P/10EVA specimen is observed. It is argued that as the sintered specimen has a higher density than the one manufactured by centrifugal casting, the sintered one is more defect-free, which can reduce strain capability. Also, it is observed that all CNT-added specimens showed an increase in their compressive strength and compressive modulus. Additionally, 1% CNT addition to the P/2EVA formulation resulted in higher compressive strain capability compared to the base P/2EVA formula. It is demonstrated that the addition of 2D fillers like CNT and MWCNT in very small amounts can enhance the regression rate of fuels due to the formation of a percolating network [24].

Tensile tests are also conducted on the specimens obtained from these fuel grains. The results are shared in Table 5.5. It is observed that the addition of CNT to the fuel has increased all tensile properties of the fuel. However, for 1% CNT addition, the result is lower tensile properties than in the 0.5% CNT-added fuel grain. It is inferred that processing conditions should be improved due to low high shear mixing time; the CNT nanoparticles may be agglomerated in the paraffinic matrix and may not perform as much as expected.

Table 5.5 Tension Test Results.

Formulation	Processing Time (Hours)	Processing Temperature (°C)	Tensile Strength [MPa]	Tensile Strain % []	Tensile Modulus [MPa]
P/2EVA_CC	-	-	3.5	2.55	150
P/2EVA_S	24	65	2.6	1.5	215
P/2EVA/0.25CNT_S	24	65	2.7	1.5	173.3
P/2EVA/0.5CNT_S	24	65	3.1	1.85	182
P/2EVA/CNT_S	24	65	2.9	1.75	200

CC: Centrifugally casted, S: Sintered

After all the aforementioned characterizations are completed, another set of parametric tests are planned to investigate the effect of the solidification phase in the mold. While the fuel is cooled at room temperature with a constant pressure and a 4-step progressive cooling profile, the number of steps, pressures, and cooling times are rearranged. P/2EVA fuel powder is placed into the mold and processed at 68°C with different combinations of pressures, step cooling profiles, and

temperatures. As a result, an improvement is gained. A fuel grain manufactured using P/2EVA powder showed 1.7 strain capability and 3.7 MPa ultimate tensile strength. This demonstrates that a higher tensile strength can be achieved by the sintering method. Additionally, the strain capability is improved to 67% of the centrifugally casted fuel grain's strain capability.

Chapter 6:
PROPULSION TEST

6.1 Experimental Setup

Combustion tests of all fuels are performed in DeltaV Space Technologies' 65mm fuel-grain small-scale test facility, as shown in Figure 6.1. In the facility, a 25-liter nitrous oxide run tank is placed on a load cell for continuous weight measurements. The flow rate throughout the firing is also collected with a Coriolis flowmeter. Pressure and temperature sensors are positioned on the run tank, line, and the motor. The data is gathered using the National Instrument CompactDaq system and recorded through the LabVIEW interface. The time sequence of the test is entered into a Raspberry Pi microcontroller, which sends a specific signal to a valve or a pyrotechnical device. Throughout the test, the pyrotechnic igniter is actuated by a 12V lithium battery, and the oxidizer is fed through the showerhead injector. After the main oxidizer valve is closed, the test motor is purged with low-pressure nitrogen gas for a couple of minutes to prevent propellant loss from the nozzle. The collected data is post-processed with MATLAB code. Rocket motor performance is predicted by MATLAB simulations running in parallel with NASA CEA to obtain thermochemical properties.

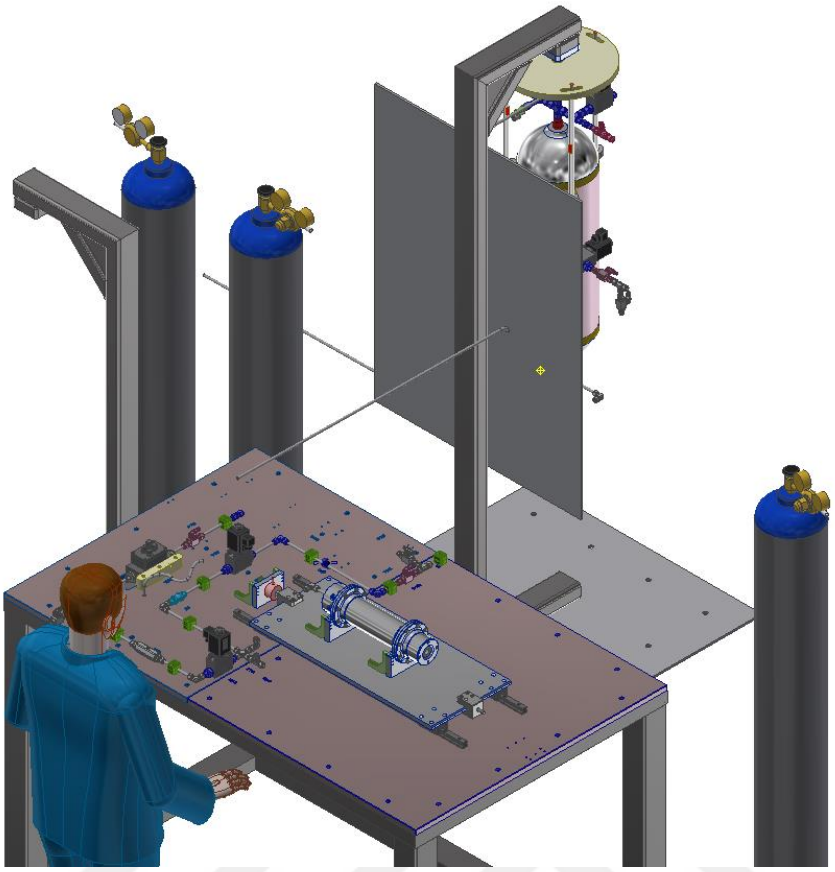

Figure 6.1 DeltaV Space Technologies 65mm lab-scale hybrid rocket research test facility demonstration.

The hybrid rocket motor used for static firing has a segmented design. The design of the rocket motor is shown in Figure 6.2 and Figure 6.3. The injector plate, fuel grain, and nozzle can be replaced ergonomically, allowing for major changes in injector, precombustion, post-combustion, and nozzle design. This setup enables firing a fuel grain with a 65mm outer diameter and varying lengths. To accommodate the required fuel length, a specific fuel casing can be machined. The segmented design of the rocket test casing allows for changing the fuel grain length by replacing the metallic case with a casing of different lengths.

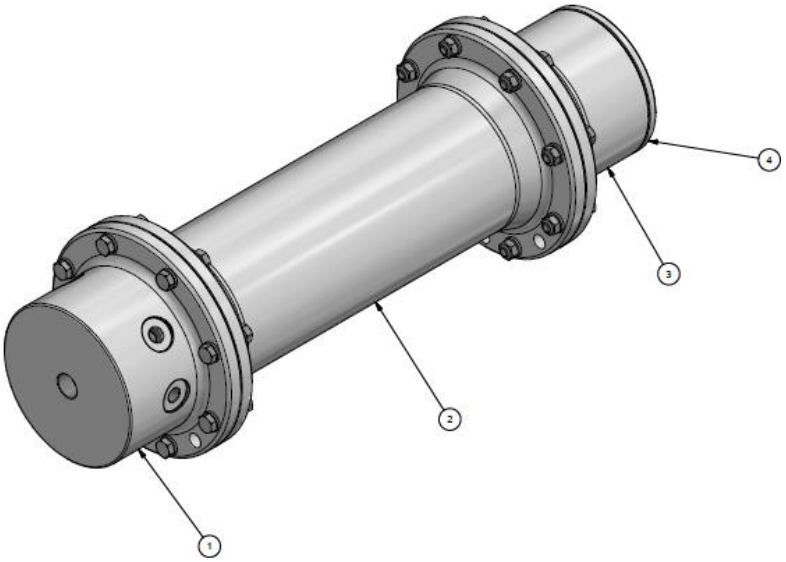

Figure 6.2 65mm fuel-sized lab-scale segmented hybrid rocket design.

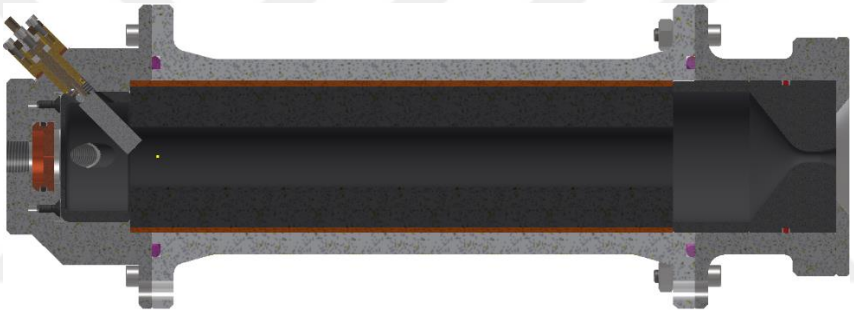

Figure 6.3 65mm fuel-size lab-scale hybrid rocket internal ballistic design.

6.2 Static Firings

As mentioned before, metallic additives provide certain advantages for hybrid rockets. In literature, it is especially highlighted that the additive size, particle coating, agglomerations, and microdefects are the most important points affecting motor performance and combustion stability. Moreover, some additives require lower temperature processing environments due to safety or performance loss issues. Five different kinds of fuel grains are manufactured for motor testing.
Firstly, Fuel grains having P/10EVA fuel formula are manufactured using both centrifugal casting and sintering methods. In addition, a 40% 3-micron sized aluminum powder doped fuel melt is prepared, and fuel grains are manufactured by direct casting into phenolic cases. To compare with the direct method, fuel grains having the same formula are manufactured using the sintering method. The atomized base fuel formula P/10EVA is mechanically mixed with 40% aluminum powder by a screw mixer and compressed in a properly sized mold. The final paraffin-based fuel formulation consists of 40% Aluminum powder, 6% EVA additives is going to be called as

P/6EVA/40Al. As another fuel formulation, fuel powder is mixed with a blowing agent at 1%, 5%, and 10% ratios using a screw mixer. These fuel formulations are going to be called as P/10EVA/1BW, P/10EVA/5BW, and P/10EVA/10BW respectively.

Regardless of the fuel manufacturing method, the fuels are placed into phenolic cases, and if the inner diameter and fuel's outer diameter have a loose tolerance, it is filled with epoxy. The weight and dimensions of each fuel grain, the epoxy amount, phenolic case weight, etc., are noted before the assembly, and the relative density of the fuel is calculated from these numbers. Then, the fuel grains are stored in vacuumed and sealed bags up to static firings.

Blowing agents are typically used in the insulation foam market and PVC market. If a blowing agent is incorporated less than 1% to PVC melt before the extrusion process, the final product has 10 to 25% less density than its virgin version. Most of the blowing agents are activated above 130°C temperature and begin to transform into gas. According to the supplied product datasheet, the blowing agent reacts below the 130°C temperature and has a density of 2730 kg/m3 in the solid phase.

In hybrid rockets, the adiabatic flame temperature may reach up to 4000K temperatures. The heat transfer and diffusive mass transfer block each other at the boundary layer and limit the regression rate for polymeric fuel grains. On the other hand, paraffin-based hybrid rocket fuels have low viscosity and surface tension promoting an unstable liquid layer at the inner surface of the fuel grain. The fuel droplets break out from the unstable fuel surface and enter the combustion zone. Karabeyoğlu et al. demonstrated and estimated the effect of vaporization and entrainment on the regression rate for different fluxes [2]. A mechanism increasing mass transfer under heat transfer dominant regimes may increase the mass transfer in a relatively low oxidizer flux zone. The addition of less than 1% any additives into the fuel formulation has an insignificant effect on the thermochemical performance of the fuel mixture. The high density and relatively low temperature required nature of blowing agents make itself a good candidate to examine its processing with the sintering method and the effect of blowing agents on ballistic performance.

Thermo-chemical calculations are conducted on each fuel formulation with changing weight fractions. From previous research thermo-chemical properties of paraffin-wax and EVA are known [26]. The heat of formation and the chemical structure of the blowing agents should be calculated. The chemical name of the blowing agent is given as sodium bicarbonate by the supplier. Its chemical structure is known. For this research, its heat of formation value is calculated by applying Benson Group Additivity Method [27]. It is calculated as -950.8 kJ/mol. O/F vs characteristic velocity graph can be seen in Figure 6.4 and the optimum points are given in Table 6.1. It should be noted that graph is prepared for 30 bar combustion pressure at vacuum. It can ben seen that Aluminum addition can provide a slight cstar performance enhancement around 2.5%.

Also, optimum O/F is shifted from 7 to 3.75. As can be expected, because of blowing agent addition in small amounts, Notable change in characteristic velocity is not observed.

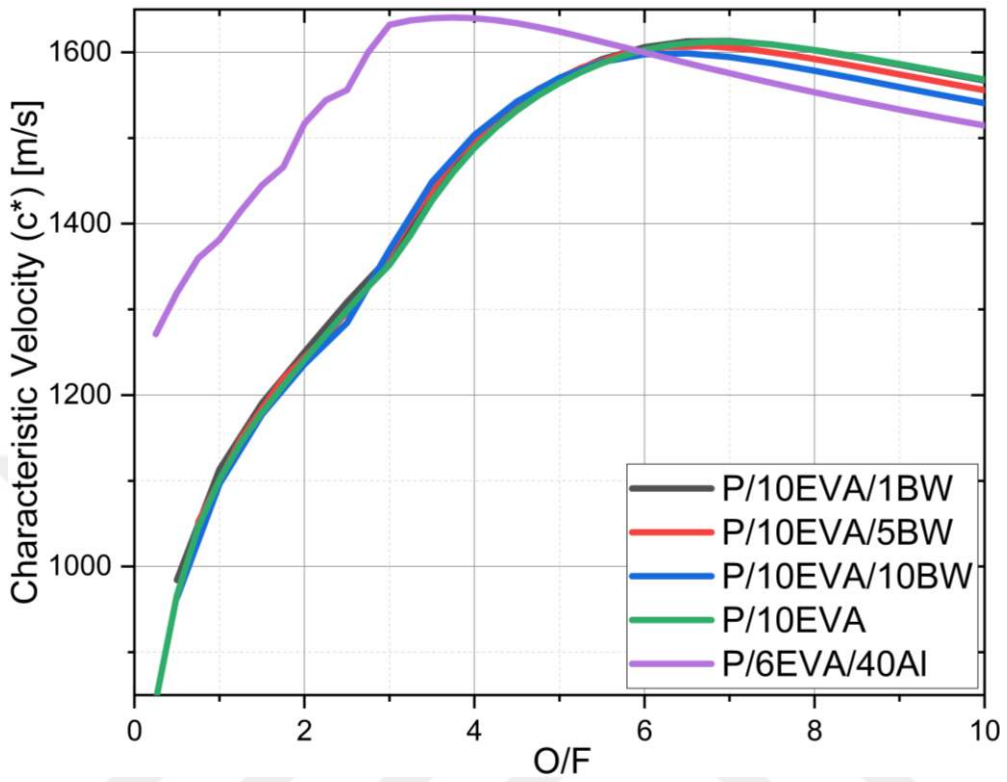

Figure 6.4 O/F vs Characteristic Velocity Graph of Fuel Formulations used throughout the research.

Tablo 6.1 Optimum O/F and cStar values of the fuel formulations used throughout the research.

Fuel Formula	**Additive**	**Addition Ratio**	**Oxidizer**	**Optimum OF**	**Cstar**
P/10EVA	EVA	10	N_2O	7	1600
P/6EVA/40Al	Aluminum	40	N_2O	3.75	1641
P/10EVA/1BW	Blowing Agent	1	N_2O	7	1613
10EVA/5BW	Blowing Agent	5	N_2O	6.75	1607
10EVA/10BW	Blowing Agent	10	N_2O	6.5	1598

6.3 Test Results

Combustion stability, combustion efficiency, and the regression rates of fuel grains are investigated in the aforementioned test motor for each fuel formulation. Paraffin-based fuel grains manufactured by centrifugal casting and sintering methods (P/10EVA), and 40% aluminum-added fuel grains (P10/6EVA/40Al) manufactured by direct casting and sintering methods are fired with 100 and 200 kg/m^{2}s oxidizer mass fluxes, respectively. The main objective of the test conduction was the investigation of combustion characteristics rather than the observation of regression rate exponents; therefore, to observe any possible abnormality, tests are repeated a couple times at the same oxidizer fluxes. Thus the reliablity of the tests are verified.

Combustion chamber pressure profile of the tests are shown in Figure 6.5. All paraffinic base fuels displayed smooth and stable combustion. This result shows that during combustion, the sintered fuel grain can survive in the combustion conditions. If any cracking or fragment rupture occurred in the fuel grain, combustion chamber pressure oscillation would be observed because of a change in fuel consumption or the possible nozzle blockage.

P/6EVA/40Al fuels, manufactured by direct casting and sintering methods, show almost the same combustion chamber pressure profile. After ignition, the test conducted with direct casting shows a slightly faster response compared to the one manufactured by the sintering method for most of the tests. It is believed that directly cast fuel has a higher paraffinic fuel to aluminum ratio compared to the sintered one. This may occur due to the agglomeration of the aluminum particles during the solidification of the paraffinic part of the fuel, but no major changes are observed. Furthermore, both paraffinic and aluminum-added fuels show very high combustion efficiency between 97% and 101%. It is believed that the calculation higher than 100% is caused by errors in the measurements. The test stand has a long oxidizer feed line, and the amount of oxidizer in the feed line after the main valve is closed affects the combustion efficiency calculations. Due to the two-phase flow in the feed line, the combustion chamber efficiency calculation is not attempted to be made more accurate because the calculated extra oxidizer amount is a function of the temperature and pressure. Almost all tests are conducted for the same burn time, resulting in all tests having a similar relative error. The error estimations are shared in Appendix A, in Chapter 10.

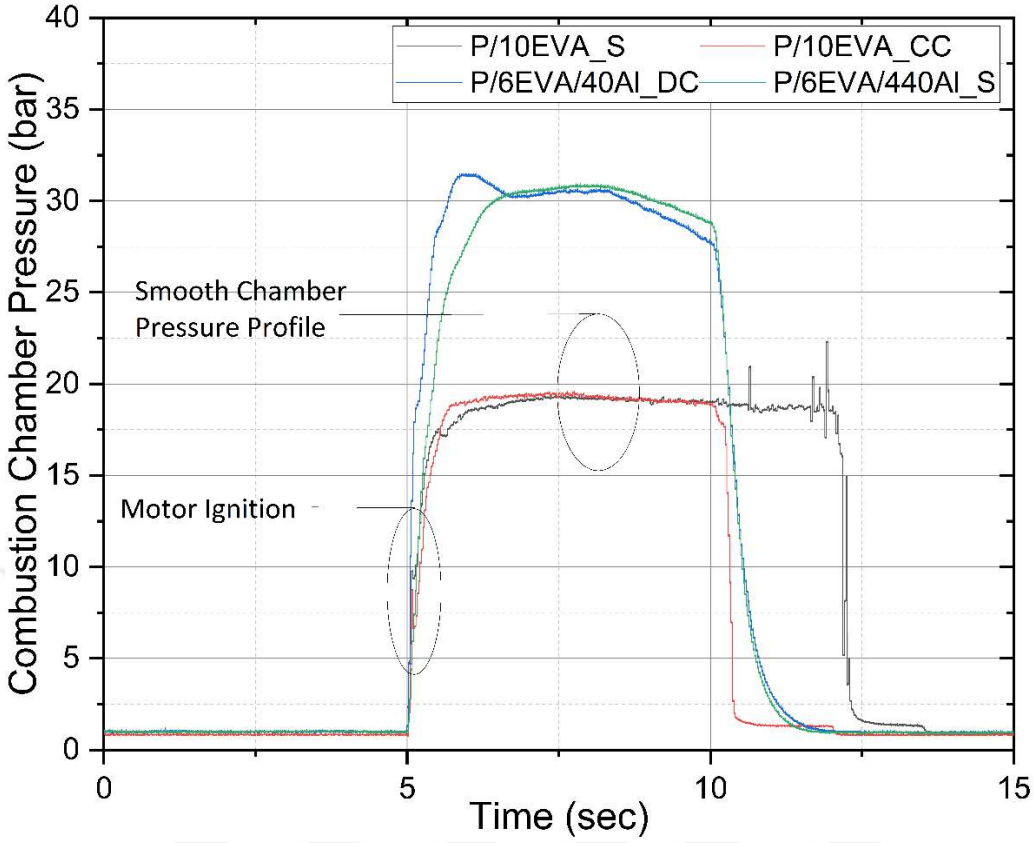

Figure 6.5 Chamber pressure profile of P/10EVA formulation and P/6EVA/40Al fuel tests.

It is observed that the tests conducted with the base fuel formula P/10EVA have very close regression rates with the Stanford reference curve [21]. However, higher regression rates are observed for some specific tests. This result may be explained by the cumulative but minimal effects of the O/F ratio and fuel length. These higher regression rate observed tests are conducted at higher O/F ratios with longer fuel grains. It is known that the O/F ratio and fuel length have a very slight effect on the regression rate of the fuel [21]. Also, a similar regression rate is observed at lower oxidizer fluxes for aluminum added fuels as can be seen in figure 6.6. 3.75mm/s and 3.5 mm/s regression rate is observed at around 120 and 200 kg/m^{2}s respectively. Parellel to previous evaluation, the tests conducted around 120kg/m2s oxidizer mass flux, is occurred at lower O/F value and longer fuel length.

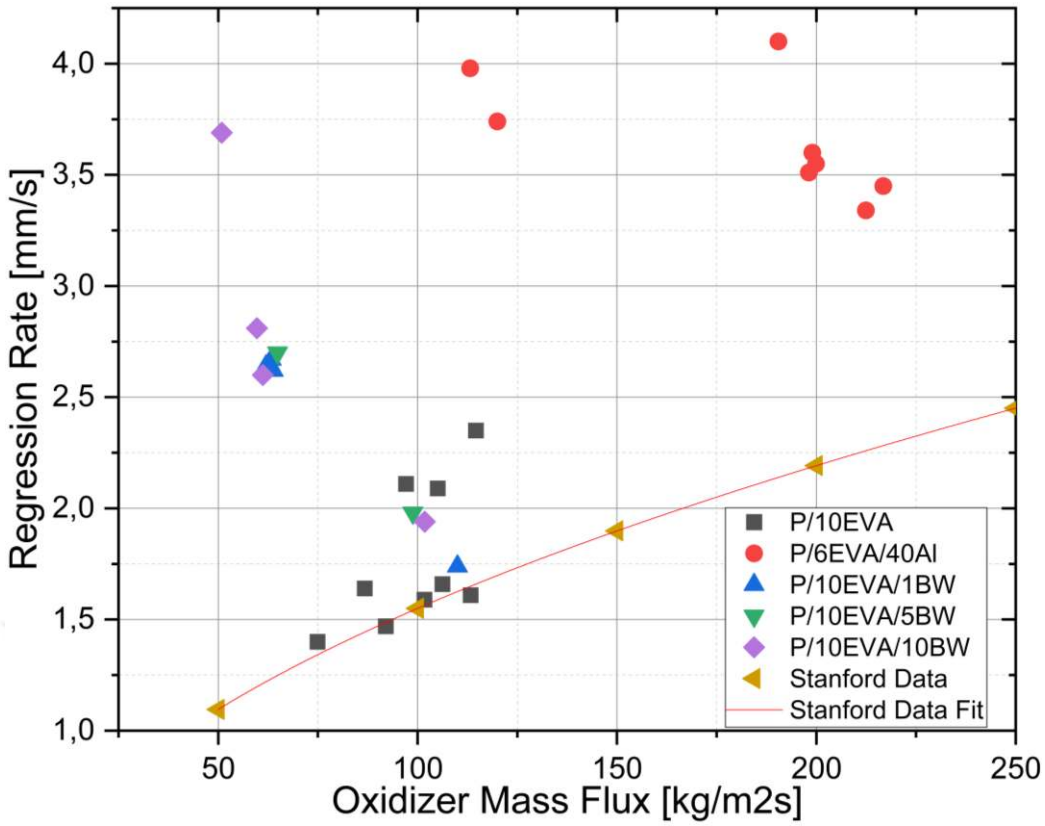

Figure 6.6 Regression rate of performed firing tests and Stanford fuel regression rate profile.

It is observed that any regression rate change between sintered fuels and compared casting methods is not observed. This result shows that sintering method provides a proper fuel grain which can handle ballistic test pressures and temperatures.

Striking results are observed from the tests conducted with fuels including different amounts of blowing agent. While the base fuel formula (P/EVA10) would be expected to have around a 1.25 mm/s regression rate, the fuels containing blowing agent show a regression rate of 2.75 mm/s at 65 kg/m^{2}s oxidizer flux. The obtained regression rate is even higher than the regression rate conducted at 100 kg/m^{2}s oxidizer flux with the base fuel formula. For the same oxidizer flux, fuel grains containing blowing agent show a 178% higher regression rate than the base fuel formula at the given reference point. Further ballistic tests at different oxidizer fluxes should be conducted, and the mechanism behind this enhancement should be investigated in detail. However, it is observed that even with 1% blowing agent mixed with the base fuel powder, the regression rate is tremendously enhanced. To make the results clear, a 10% blowing agent fuel and the base fuel formula are tested on the same day, one after another. GMT146, GMT147, and GMT149 are conducted one after another to arrange the oxidizer fluxes to approximate each other. GMT148 test data is evaluated as misleading due to the burn-through caused by the minimal crack throughout the fuel grain. Tests conducted on the same day indicate the same enhancement in the

regression rate.

The mass transfer mechanism can be enhanced by reducing the effective heat of gasification, decreasing the blocking factor in the boundary layer, and increasing heat transfer [2]. Carmicino et. al. proposed a model to characterize the boundary layer of any neat paraffin formulation. According to the model and the conducted tests, the surface temperature of a fuel grain made of paraffin wax having 32 carbons on the backbone has 770±20°C with gaseous oxygen [23]. As nitrous oxide has a higher adiabatic flame temperature than gaseous oxygen with paraffin wax, the expected surface temperature is higher than the value. In other words, the liquid layer has a sufficient temperature for blowing agent decomposition. I propose that the high amount of gasification in the liquid layer may not only promote the droplet entrainment throughout the combustion zone but also it may increase the Reynolds number at the surface due to the perpendicular flow contribution to the main flow direction. The parameters affecting the heat and mass transfer at the boundary layer and its possible outcomes are detailed in Karabeyoğlu et. al.'s article [2]. I propose that the effect of the blowing agent at higher oxidizer fluxes may be diminished due to getting a thinner liquid layer. Also, the decomposition rate of the blowing agent may not be as fast as the droplet entrainment. The effect of the blowing agent may be more dominant in entrainment weak, low oxidizer flux regions. Further investigation should be conducted to understand the mechanism of the behind. As a result of such new fuel grain manufacturing method gave a chance to evaluate these additives as a possible constituent to arrange regression rate of fuels.

Table 6.1 Firing test results.

Test	Manufacturing Method	Fuel Formulation	Fuel Relative Desnsity (%)	Burn time (sec)	Chamber Pressure (bar)	Oxidizer Mass Flow rate (g/sec)	Average Oxidizer Flux (g/cm2s)	Regression Rate (mm/s)	O/F []	C* Efficiency (%)	NOTES:
GMT59	CC	P/10EVA	99.4	10	29.8	199.1	113.3	1.61	3.64	0.995	
GMT60	CC	P/10EVA	99.5	10	24.8	194	106	1.66	3.36	1.01	
GMT74	CC	P/10EVA	99.6	8	21.6	166.1	92	1.47	3.32	1.02	
GMT121	S	P/10EVA	99.7	7	20.1	148.7	101.7	1.59	1.81	0.9	
GMT125	S	P/10EVA	99.7	7	18.7	166.8	97.1	2.11	3.88	0.88	
GMT126	CC	P/10EVA	99.8	7	23.5	179.2	105	2.09	4.22	0.99	
GMT127	CC	P/10EVA	99.7	5	22.3	172.4	114.6	2.35	3.84	0.99	
GMT131	DC	P/6EVA/40Al	99.5	5	32	236.4	216.8	2.38	4.89	0.94	
GMT132	DC	P/6EVA/40Al	99.2	5	29.1	250.8	190.5	4.1	3.81	0.81	
GMT133	S	P/6EVA/40Al	99.5	5	27.43	176.4	148.9	3.77	3.2	0.99	
GMT134	DC	P/6EVA/40Al	99.1	5	29.4	229	212.4	3.34	4.71	0.94	
GMT135	S	P/6EVA/40Al	99.5	5	29	225.8	199	3.6	4.41	0.92	
GMT136	S	P/6EVA/40Al	99.5	5	26.2	223.9	199.9	3.55	4.46	0.84	

Test	Manufacturing Method	Fuel Formulation	Fuel Relative Desnsity (%)	Burn time (sec)	Chamber Pressure (bar)	Oxidizer Mass Flow rate (g/sec)	Average Oxidizer Flux (g/cm2s)	Regression Rate (mm/s)	O/F []	C* Efficiency (%)	NOTES:
GMT137	S	P/6EVA/40Al	99.6	5	28.6	219	198.1	3.51	4.23	0.93	
GMT138	S	P/6EVA/40Al	99.8	8	32.6	-	-	-	-	-	
GMT139	S	P/6EVA/40Al	99.7	5	29.6	100	59.7	2.81	2.41	0.77	Chamber pressure tranducer fail
GMT140	S	P/10EVA/5BW	99.7	5	28.2	106.3	64.9	2.7	2.88	0.72	Chamber pressure tranducer fail
GMT141	S	P/10EVA/5BW	99.7	5	-	-	-	1.93	-	-	Partially data loss
GMT142	S	P/10EVA/1BW	99.6	5	-	102.8	63.8	2.62	2.94	-	Chamber pressure tranducer
GMT143	S	P/10EVA/1BW	99.6	5	-	103	63.3	2.67	2.93	-	Chamber pressure tranducer fail

Test	Manufacturing Method	Fuel Formulation	Fuel Relative Desnsity (%)	Burn time (sec)	Chamber Pressure (bar)	Oxidizer Mass Flow rate (g/sec)	Average Oxidizer Flux (g/cm2s)	Regression Rate (mm/s)	O/F []	C* Efficiency (%)	NOTES:
GMT144	S	P/10EVA/1BW	99.7	5	-	100.3	62	2.64	2.93	-	Chamber pressure tranducer fail
GMT145	S	P/10EVA/1BW	99.7	5	-	98	61.2	2.6	2.58	-	Chamber pressure tranducer fail
GMT146	CC	P/10EVA	96.9	5	33.6	110	86.7	1.64	5.9	0.83	
GMT147	CC	P/10EVA	97	8	29.6	109.5	74.9	1.4	6.5	0.79	
GMT148	CC	P/10EVA	97	5	27.3	60	59.4	3.2	2.23	1.01	Unproper data due cracked fuel testing
GMT149	S	P/10EVA/10BW	97.6	5	24.6	59	50.9	2.61	1.65	0.99	

P/10EVA: Paraffin Wax + 10% EVA *P/10EVA/1BW: Paraffin Wax + 10% EVA + 1% Blowing Agent*

P/6EVA/40Al: Paraffin Wax + 10% EVA + 40% Aluminum *P/10EVA/5BW: Paraffin Wax + 10% EVA + 5% Blowing Agent*

P/10EVA/10BW: Paraffin Wax + 10% EVA + 10% Blowing Agent

Chapter 7:
SYSTEM COMPARISON AND RESULTS

Both centrifugal casting and direct casting are widely used conventional methods for manufacturing paraffin-based fuel grains. Centrifugal casting is the ideal choice for those who want to obtain mechanical properties close to the formulation characteristics when the fuel formulation consists of only polymeric ingredients. However, if the fuel formulation includes any high-density additive, centrifugal casting is not suitable for manufacturing the fuel grain.

On the other hand, direct casting has been the primary method for obtaining a fuel grain for a long time. However, direct casting leads to broad dimensional changes, uneven additive distribution, and the formation of micro voids and cracks on any scale. These are commonly observed faults associated with direct casting. The proposed method can be considered an alternative method, especially for direct casting, addressing some of the drawbacks of the traditional direct casting approach.

7.1 *Advantages in different aspects compared to conventional methods*.

When comparing the proposed sintering method with conventional centrifugal casting, the sintering method offers distinct advantages for specific missions. One significant advantage is that the fuel grain can be manufactured at any inner port diameter, which is not feasible with centrifugal manufacturing due to the high risk of thermal cracking when the inner port diameter exceeds a 1:2 ratio. This flexibility in the inner port diameter allows for higher volumetric loading in a hybrid rocket.

Furthermore, when comparing it to the direct casting method, sintering enables the consistent manufacturing of the same quality fuel grain each time. The formation of voids, cracks, or agglomeration is very sensitive to processing temperatures. The proposed method provides an opportunity to mix neat paraffin wax with aluminum particles theoretically without any viscosity-increasing constituent and without agglomeration.

Additionally, the sintering method allows for the addition of various additives through solid-phase mixing. This means that additives with high hydrophilic properties, or high loading required for fuel formulations providing hypergolicity, can be processed without any doubt. High-density

metallic additives or those with very low decomposition temperatures can be easily incorporated into the formulation. Despite the addition of these additives, the sintering method ensures consistent mechanical properties, homogeneous material content, and high relative density in the fuel grain.

Chapter 8:
CONCULUSION AND FINAL REMARKS

The proposed sintering method marks the beginning of a breakthrough. It has the potential to meet mission-specific needs. In this study, various fuel powder manufacturing methods are proposed. For industrial production purposes, a fuel powder manufacturing reactor is designed, and many fuel grains are sintered from the powder produced by the designed reactor. Different mold designs are evaluated through Ansys analysis to obtain uncracked fuel grains. The study investigates sintering process parameters and their effects on fuel grain mechanical properties and micro-scale characteristics. Fuel grains manufactured with different sintering parameters are machined to obtain mechanical test specimens. As a result of process optimization, P/2EVA formulation's strain capability manufactured by the sintering method is enhanced, reaching up to 70% of the fuel grains manufactured by the centrifugal casting method. The same tensile strength is obtained from both the specimens taken from both methods.

The study infers the triggering of four different mechanisms. Firstly, heating the material allows thermoplastic material diffusion, entangling chains at the trans-particular surfaces. Secondly, these contact surfaces among powder particles may be strengthened by the addition of 2D and 3D fillers. Thirdly, the fuel grain can be heated just above its melting peak temperature for a short period of time. It should be noted that mold design and solidification processes directly affect the mechanical properties of the final fuel grain. Lastly, a fuel formulation having a super-cooling window can be arranged by modifying the continent materials. In the research, 2D filler, CNTs, is added to the P/2EVA formulation during atomization, and fuel powders are processed under the same conditions. It is observed that the addition of CNT to the base fuel powder enhances its mechanical properties. Additionally, a common high-density metallic additive is mixed with the base fuel formula P/10EVA and fired on a hybrid rocket. No significant differences are observed in terms of fragment generation or manufacturing methods during firing tests. Moreover, a temperature-sensitive material blowing agent is evaluated as a hybrid rocket fuel additive. Fuel grains loaded with 1-5% and 10% blowing agent are produced using the sintering method. The regression rates of these formulations are investigated through firing tests. It is observed that the regression rates of the fuels are enhanced in every case blowing agent added fuel formulations. Particularly, at 50kg/m2s oxidizer flux, the regression rate of the base fuel increases by 178%. Some clues suggest that as the oxidizer mass flux increases, the regression rate of the blowing agent-added fuels approaches the base formulation regression characteristic.

Chapter 9:
FUTURE WORKS

In future studies, it is important to investigate whether different kinds of paraffin wax-based fuel formulations have a super-cooling window. Particularly, fuel formulations containing macrocrystalline waxes may exhibit a super-cooling window, and processing the fuel grain within this temperature range using the last mold configuration could potentially result in a very close strain capability compared to centrifugally casted fuel grains. Another significant area of research is the exploration of 2D and 3D fillers that can be homogenously dispersed using the sintering method. The impact of these additives on fuel grain performance should be thoroughly explored to contribute valuable insights to the existing literature. Furthermore, the firing tests have indicated enhanced regression rates for fuel formulations with blowing agents. To fully understand and optimize this effect, it is essential to carefully investigate regression rate exponents and combustion efficiencies in future studies.

Chapter 10:
APPENDIX

10.1 APPENDIX A

It is important to know the systematic error caused by source of measurements in the test set up. Karabeyoğlu bring together all the errors to estimate the random error according to error analysis methodology [25].

Specifically, in this study, firing tests and mechanical tests are conducted. Regression rate of fuel grains are calculated with respect to a specific oxidizer mass flux shared in Table 6.1. The regression rate error and oxidizer mass flux error can be calculated according to the given formulas below:

$$E_{\dot{r}} = \sqrt{\left(\frac{R}{R-1}E_{D_f}\right)^2 + \left(\frac{1}{R-1}E_{D_i}\right)^2 + E_{t_b}^2}$$

$$E_{GOX} = \sqrt{\left(\frac{2R}{R-1}E_{D_f}\right)^2 + \left(\frac{2}{R-1}E_{D_i}\right)^2 + E_{\dot{m}_{ox}}^2}$$

R response to Df/Di and errors caused by initial and final inner diameter should be considered for both regression rate and oxidizer mass relative error calculations. All fuel grains are accurately machined by turning and drilling operations. The initial inner diameter is precisely measured. The final inner diameter after firing test are assumed by the mass measurements occurred before and after the firing test; therefore, the assumption of the final diameter is effected by the measurement of outer & inner diameter, length and mass measurements. Final diameter of error can be calculated as:

$$E_{D_f} = 0.5\ x\ \left(1 + \frac{D_i}{D_f}\right) x\ \sqrt{E_{\Delta M}^2 + E_{\rho}^2 + E_L^2}$$

To observe the expected maximum error for the firing tests, the minimum initial port diameter 20mm and maximum possible final diameter 65mm is accepted. 0.01 relative error is predicted for both mass and length measurements. Relative density error is assumed as 0.025 conservatively. Also, it is known that the valves using in test set up have around 0.1sec response time. Relative

burn time error is assumed as 0.04. The flowrate is measured by Honeywell Coriolis flowmeter, its accuracy is given as 0.65% in the worst scenario. The relative oxidizer mass flowrate calculation is defined as:

$$E_{\dot{m_{ox}}} = \sqrt{E_{CFM}^2 + 0.5E_{temp}^2}$$

Relative CFM error is assumed as 0.065 and relative temperature error is neglected.
As a result of calculations, relative random regression rate error is calculated as 0.049mm/s and relative random oxidizer mass flux error is calculated as 0.085 kg/m2s in the worst case.

10.2 APPENDIX B

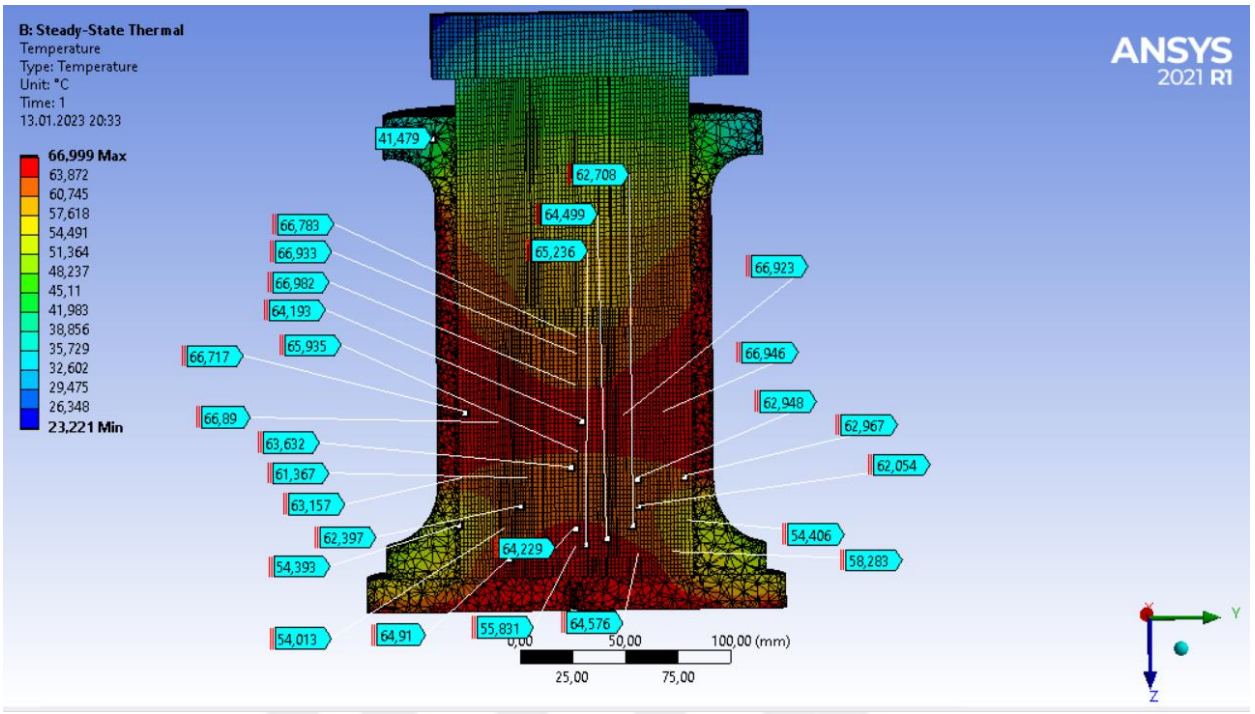

Figure 10.1 Configuration 1

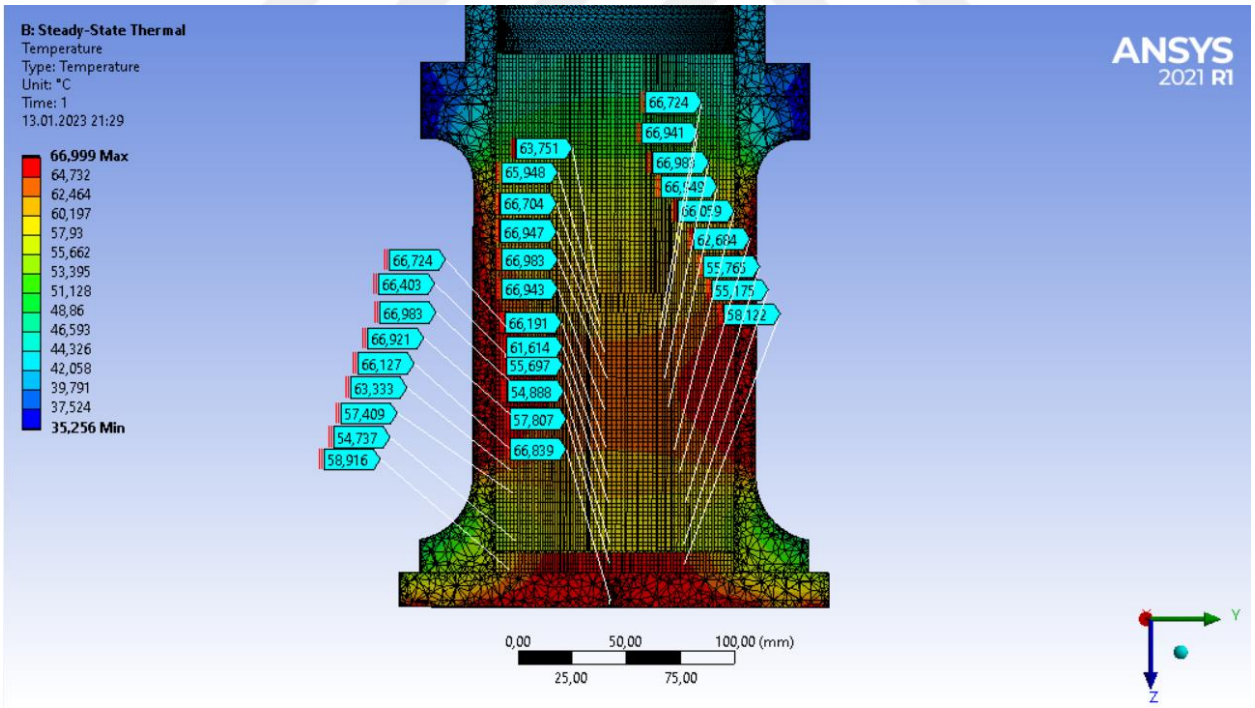

Figure 10.2: Configuration 2

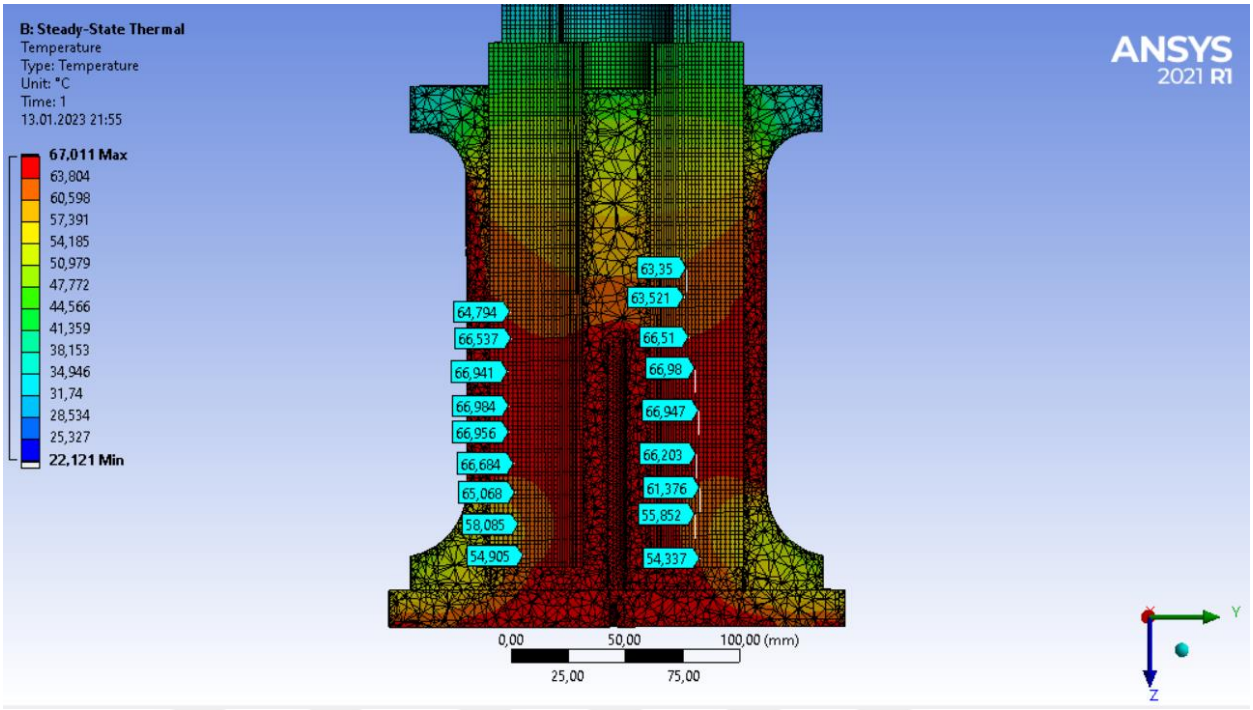

Figure 10.3: Configuration 3

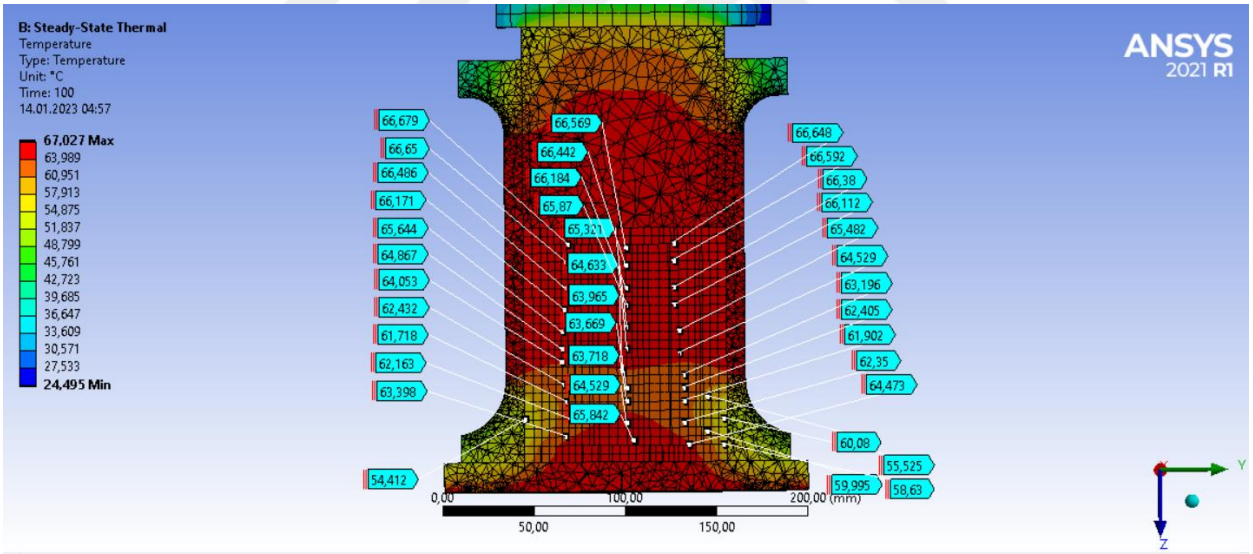

Figure 10.4: Configuration 4

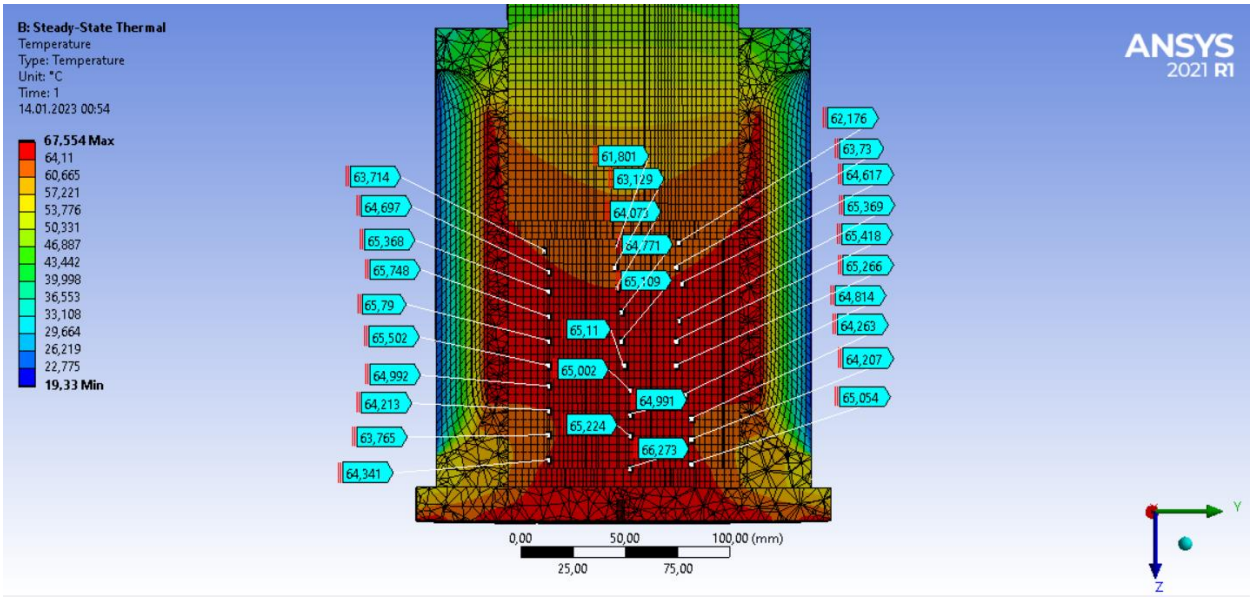

Figure 10.5: Configuration 5

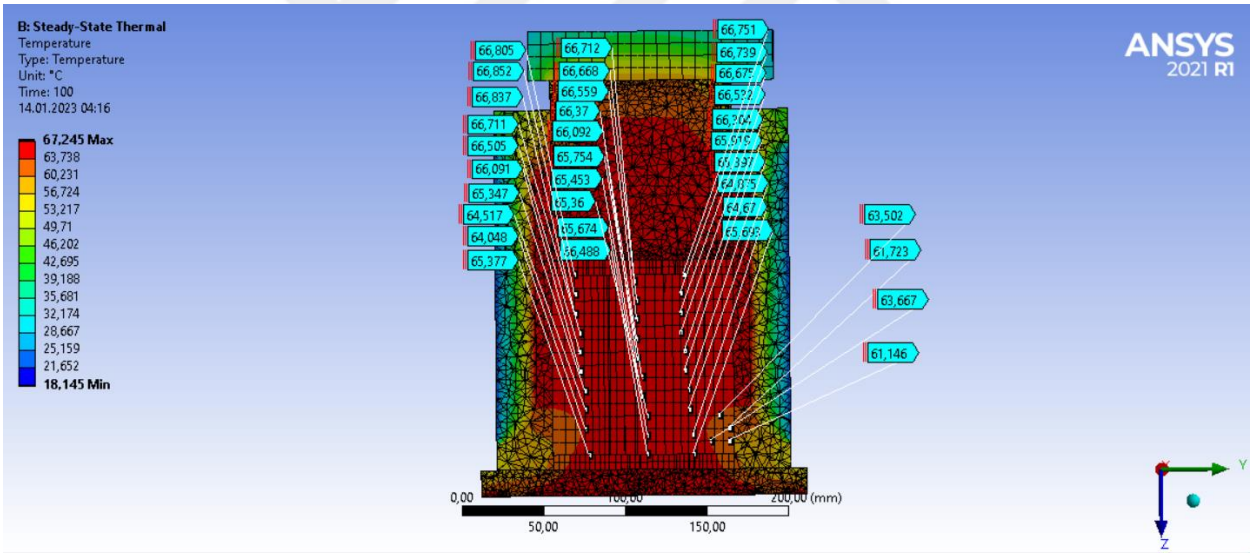

Figure 10.6: Configuration 6

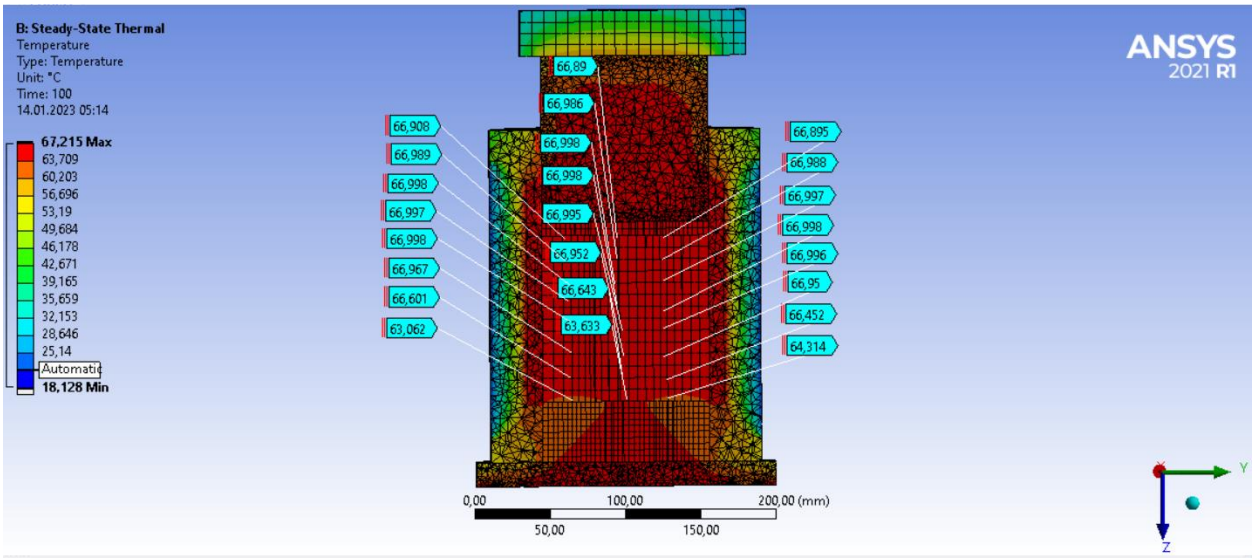

Figure 10.7: Configuration 7

Chapter 11:
BIBLIOGRAPHY

---

[1] Cantwell, Brian, et al. “Recent Advances in Hybrid Propulsion.” *International Journal of Energetic Materials and Chemical Propulsion*, vol. 9, no. 4, 2010, pp. 305–326., doi:10.1615/intjenergeticmaterialschemprop.v9.i4.20.

[2] Karabeyoglu, M., et al. “Development and Testing of Paraffin-Based Hybrid Rocket Fuels.” *37th Joint Propulsion Conference and Exhibit*, 2001, doi:10.2514/6.2001-4503.

[3] Armold, Derrick, et al. “Test of Hybrid Rocket Fuel Grains with Swirl Patterns Fabricated Using Rapid Prototyping Technology.” *49th AIAA/ASME/SAE/ASEE Joint Propulsion Conference*, 2013, doi:10.2514/6.2013-4141.

[4] Paccagnella, Enrico, et al. “Scaling Parameters of Swirling Oxidizer Injection in Hybrid Rocket Motors.” *Journal of Propulsion and Power*, vol. 33, no. 6, 2017, pp. 1378–1394., doi:10.2514/1.b36241.

[5] Merotto, L.; Boiocchi, M.; Mazzetti, A.; Maggi, F.; Galfetti, L.; De Luca, L.T. Characterization of a family of para_n-based solid fuels. In Proceedings of the 4th European Conference for Aerospace Sciences (EUCASS), St. Petersburg, Russia, 4–8 July 2011.

[6] Mazzetti, Alessandro, et al. “Paraffin-Based Hybrid Rocket Engines Applications: A Review and a Market Perspective.” *Acta Astronautica*, vol. 126, 2016, pp. 286–297., doi:10.1016/j.actaastro.2016.04.036.

[7] Masato, Davide, et al. “Prototyping and Modeling of the Centrifugal Casting Process for Paraffin Waxes.” *Materials and Manufacturing Processes*, vol. 32, no. 16, 2017, pp. 1823–1830., doi:10.1080/10426914.2017.1317791.

[8] Kumar, Rajiv, and Periyapatna A. Ramakrishna. “Studies on Eva-Based Wax Fuel for Launch Vehicle Applications.” *Propellants, Explosives, Pyrotechnics*, vol. 41, no. 2, 2016, pp. 295–

303., doi:10.1002/prep.201500172.

[9] Kim, Soojong, et al. “Effect of Paraffin-LDPE Blended Fuel on the Hybrid Rocket Motor.” *46th AIAA/ASME/SAE/ASEE Joint Propulsion Conference & Exhibit*, 2010, doi:10.2514/6.2010-7031.

[10] Mengu, Dinesh, and Rajiv Kumar. “Development of EVA-Sebs Based Wax Fuel for Hybrid Rocket Applications.” *Acta Astronautica*, vol. 152, 2018, pp. 325–334., doi:10.1016/j.actaastro.2018.08.034.

[11] Kobald, Mario, and Elena Toson. “Evaluation of Paraffin-Based Fuels for Hybrid Rocket Engines.” *50th AIAA/ASME/SAE/ASEE Joint Propulsion Conference*, 2014, doi:10.2514/6.2014-3646.

[12] Armold, Derrick M., et al. “Testing of Hybrid Rocket Fuel Grains at Elevated Temperatures with Swirl Patterns Fabricated Using Rapid Prototyping Technology.” *50th AIAA/ASME/SAE/ASEE Joint Propulsion Conference*, 2014, doi:10.2514/6.2014-3754.

[13] Veale, Kirsty, et al. “A Review of the Performance and Structural Considerations of Paraffin Wax Hybrid Rocket Fuels with Additives.” *Acta Astronautica*, vol. 141, 2017, pp. 196–208., doi:10.1016/j.actaastro.2017.10.012.

[14] Bisin, Riccardo, et al. “A New Strategy for the Reinforcement of Paraffin-Based Fuels Based on Cellular Structures: The Armored Grain — Mechanical Characterization.” *Acta Astronautica*, vol. 176, 2020, pp. 494–509., doi:10.1016/j.actaastro.2020.07.003.

[15] Piscitelli, F., et al. “Characterization and Manufacturing of a Paraffin Wax as Fuel for Hybrid Rockets.” *Propulsion and Power Research*, vol. 7, no. 3, 2018, pp. 218–230., doi:10.1016/j.jppr.2018.07.007.

[16] Chen, S., Tang, Y., Zhang, W., Shen, R., Yu, H., Ye, Y., & DeLuca, L. T. (2019). Innovative methods to enhance the combustion properties of solid fuels for hybrid rocket propulsion. *Aerospace*, *6*(4), 47. https://doi.org/10.3390/aerospace6040047

[17] Akhter, Md. Z., & Hassan, M. A. (2020). Energetic additives for hybrid rocket propulsion - review. *2020 Advances in Science and Engineering Technology International Conferences (ASET)*. https://doi.org/10.1109/aset48392.2020.9118206

[18] Jobin, O., Mottillo, C., Titi, H. M., Marrett, J. M., Arhangelskis, M., Rogers, R. D., Elzein, B., Friščić, T., & Robert, É. (2021). *Metal-Organic Frameworks as Hypergolic Additives for Hybrid Rockets*. https://doi.org/10.33774/chemrxiv-2021-v6ggv

[19] Rang, S., Jeong, J., Khandu Bhosale, V., & Kwon, S. (2022). Reactivity of hypergolic hybrid solid fuel with industrial grade hydrogen peroxide. *Fuel*, *330*, 125543. https://doi.org/10.1016/j.fuel.2022.125543

[20] Benhidjeb-Carayon, A., Gabl, J., & Pourpoint, T. L. (2018). Hypergolic ignition and relights of a paraffin-based hybrid grain. *2018 Joint Propulsion Conference*. https://doi.org/10.2514/6.2018-4661

[21] Karabeyoglu, A., Zilliac, G., Cantwell, B. J., DeZilwa, S., & Castellucci, P. (2004). Scale-up tests of high regression rate paraffin-based hybrid rocket fuels. *Journal of Propulsion and Power*, *20*(6), 1037–1045. https://doi.org/10.2514/1.3340

[22] Karabeyoğlu, A. (2016). Performance additives for Hybrid Rockets. *Chemical Rocket Propulsion*, 139–163. https://doi.org/10.1007/978-3-319-27748-6_5

[23] Carmicino, C., Gallo, G., & Savino, R. (2021). Self-consistent surface-temperature boundary condition for liquefying-fuel-based hybrid rockets internal-ballistics simulation. *International Journal of Heat and Mass Transfer*, *169*, 120928. https://doi.org/10.1016/j.ijheatmasstransfer.2021.120928

[24] Bokobza, L., & Belin, C. (2007). Effect of strain on the properties of a styrene–butadiene rubber filled with multiwall carbon nanotubes. *Journal of Applied Polymer Science*, *105*(4), 2054–2061. https://doi.org/10.1002/app.26153

[25] Karabeyoglu, A., Cantwell, B., & Zilliac, G. (2005). Development of scalable space-time averaged regression rate expressions for hybrid rockets. *41st AIAA/ASME/SAE/ASEE Joint Propulsion Conference &Amp; Exhibit*. https://doi.org/10.2514/6.2005-3544

[26] Bilge, K., Kokal, U., Emerce, N. B., Yildiz, U. C., Baysal, M., & Karabeyoglu, A. (2019). Selection criteria for tackifier addition to paraffin wax based hybrid rocket fuels. *AIAA Propulsion and Energy 2019 Forum*. https://doi.org/10.2514/6.2019-3921

[27] Benson, S. W. (1965). III - bond energies. *Journal of Chemical Education*, *42*(9), 502. https://doi.org/10.1021/ed042p502